

# A Gaussian process and linear-based method for computing cut distributions in modular Bayesian calibration of two chained computer models

Oumar Baldé<sup>\*†</sup>    Guillaume Damblin<sup>\*‡</sup>    Amandine Marrel<sup>§¶</sup>

Antoine Bouloré<sup>||</sup>    Loïc Giraldi<sup>||</sup>

March 17, 2026

## Abstract

Computer models are widely used in science and engineering to simulate complex systems. However, these models are affected by several sources of uncertainty, which may limit their use for decision making in risk management. We present a Bayesian approach for quantifying parameter uncertainty in a chain of two computer models motivated by multiphysics simulations in the nuclear field. Part of the inputs of a downstream model parametrized by  $\theta \in \mathbb{R}^p$  come from the outputs of an upstream model parametrized by  $\lambda \in \mathbb{R}^q$ . Usually, the joint posterior distribution of  $(\theta, \lambda)$  would be obtained by applying Bayes' theorem using the experimental observations of both models. However, when the observations of the downstream model are too indirect to provide informative inference on  $\lambda$ , it may be preferable to compute a modular posterior distribution of  $(\theta, \lambda)$ , referred to as the *cut distribution*. Assuming that the posterior distribution of  $\lambda$  has been previously estimated from observations of the upstream model only, we aim to compute the posterior distribution of  $\theta$  conditional on  $\lambda$  using observations from the downstream model. To this end, we propose a Gaussian-process and linear-based framework to estimate the functional dependence between  $\theta$  and  $\lambda$ , denoted by  $\theta(\lambda)$ , where each component is modeled as a realization of a Gaussian process. As the downstream model is approximated by a linear function of  $\theta(\lambda)$ , Bayesian conjugacy allows us to derive a Gaussian posterior predictive distribution of  $\theta(\lambda)$  for any realization of  $\lambda$ . The effectiveness of the method is illustrated through several synthetic examples, and we highlight how variations in  $\lambda$  impact the predictive distribution of the chained simulation.

---

<sup>\*</sup>Université Paris-Saclay, CEA DES, Service de Génie Logiciel pour la Simulation, 91190, Gif-sur-Yvette, France

<sup>†</sup>Institut de Mathématiques de Toulouse, Université Paul Sabatier, 118 Route de Narbonne, 31062 Toulouse. Oumar Baldé is currently a post-doctoral researcher at CEA, DES, IRESNE, DER, SESI.

<sup>‡</sup>Corresponding author. (guillaume.damblin@cea.fr).

<sup>§</sup>CEA DES, IRESNE, DER, SESI, Cadarache, 13108 St-Paul-Lez-Durance, France

<sup>¶</sup>LMA, Université d'Avignon, 84140 Avignon, France

<sup>||</sup>CEA DES, IRESNE, DEC, SESC, Cadarache, 13108 St-Paul-Lez-Durance, France

**Keywords.** Bayesian calibration, cut distribution, chained models, Gaussian process.  
**AMS classification:** 60G15, 62F15, 62G08.

## 1 Introduction

Numerical simulations have become essential for understanding, analyzing, and predicting complex systems and phenomena in all areas of engineering and science [40]. Indeed, when real field experiments are too costly or impossible to conduct for technical or ethical reasons, they are replaced by numerical counterparts that have benefited from a huge increase in computational resources over the last thirty years. However, the physical models and equations underlying the simulations are affected by various sources of uncertainty [22] that can affect the robustness of numerical predictions for decision-making. One of the most critical uncertainties is known as parameter uncertainty, which arises when a numerical simulation depends on a number of uncertain tuning or calibration parameters [18]. One popular way of inferring such parameters is Bayesian calibration using available experimental observations [41]. Bayesian calibration computes probability distributions for the uncertain parameters, unlike deterministic calibration, which provides a single best-fitting value [7].

This paper contributes to Bayesian calibration in the particular context of multiphysics simulations where several computer models of different physics are connected to one another to simulate the entire phenomenon of interest. As part of fuel simulations for nuclear power plants, we are interested in a multiphysics solver named ALCYONE [19], which is composed of interlinked models that represent the mechanical, thermal, and chemical behaviors of fuel rods in the core of pressurized water reactors. Recently, some papers have addressed forward uncertainty propagation for such multiphysics simulations in the nuclear field [15, 45, 1]. Other works have dealt specifically with the emulation of a chain of several computer models via different strategies relying on Gaussian processes [23, 39, 33]. For our part, we present a methodological contribution to Bayesian calibration for a chain of two models integrated into the ALCYONE solver. Specifically, we are interested in the fission gas behavior model, which takes as input the output of the thermal model. The latter simulates the evolution of the temperature within the fuel rod during the fission reaction and provides as output the associated temperature field. Then, the fission gas behavior model, as a function of the thermal model, continuously represents the behavior of the fission products (fuel swelling and release of fission gas atoms) during the fission reaction. Figure 1 displays the two models in blue within the global multiphysics calculation workflow: the thermal model depends on the conductivity parameter  $\lambda \in \Lambda \subset \mathbb{R}^q$  (here  $q = 1$ ) and the fission gas behavior model depends on the parameter  $\theta \in \mathcal{T} \subset \mathbb{R}^p$  ( $p \geq 1$ ).

In the literature, several approaches have been proposed for quantifying parametric uncertainties in such a chain of numerical models. First of all, there is the full modeling approach, which naturally conducts a simultaneous calibration of the two sets of parameters using all the available experimental data related to both models [14, 30]. It has the advantage of dealing with all the uncertainties together, coherently, and using

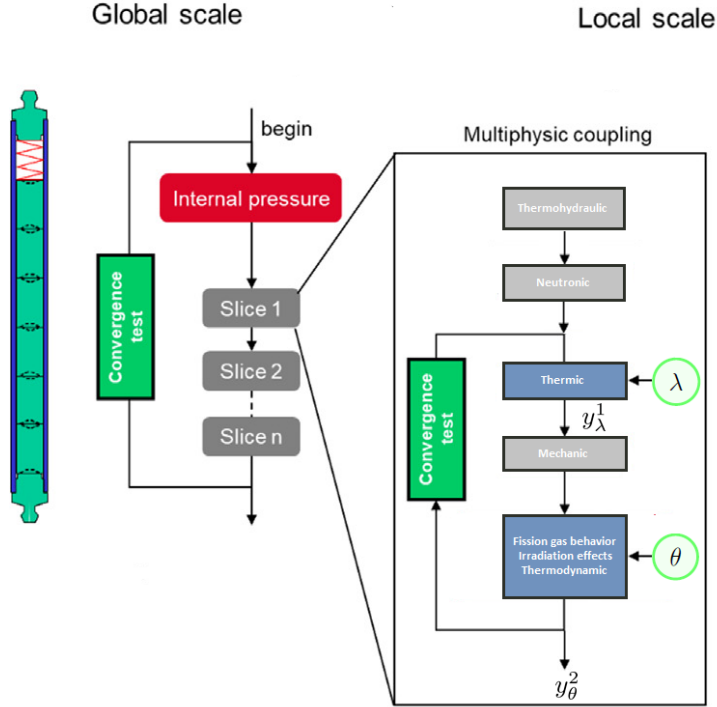


Figure 1: Chaining of the thermal and fission gas behavior models of the ALCYONE solver [19]:  $\lambda$  is the thermal conductivity and  $\theta$  represents the parameters of the fission gas behavior model.

all available information. However, as pointed out and illustrated in [21], the combination of several sources of information might lead to a misleading quantification of uncertainties. This happens, for example, when the observations of the downstream model are considered to be too indirect to bring valuable information for the posterior uncertainty of the parameters of the upstream model. An alternative is then to consider a two-stage calibration approach such as the segmented calibration [14, 44] or the cut distribution [36, 21]. In these approaches, the parameters  $\theta$  of the downstream model and the parameter  $\lambda$  of the upstream model are, in a certain sense, calibrated separately with experimental observations representative of each model. Being unable to capture any statistical dependence between  $\theta$  and  $\lambda$ , the segmented calibration may, however, inflate the predictive uncertainty of the downstream model. The cut distribution does not suffer from this limitation and, moreover, comes with statistical support that it may outperform the full posterior in certain settings. This typically occurs when some data bring information suspected to be not reliable enough because of model misspecification or lack of identifiability. Using such data may actually lead to lower predictive scores than those computed with a cut posterior [21]. Note that the latter distribution falls within modular Bayesian calibration approaches, as discussed originally in Liu et al. [25].

In this work, we aim to compute the cut distribution for quantifying the joint poste-

rior uncertainty of  $\theta$  and  $\lambda$ . On top of the previous discussion, choosing this framework is driven by the fuel application where a marginal posterior distribution of  $\lambda$  was computed from an earlier calibration study based on the observations of the thermal model only. More importantly, this distribution has been validated by the fuel experts who developed the ALCYONE solver. Therefore, we focus on the conditional distribution of  $\theta$  given  $\lambda$ , denoted  $\mathbb{P}_{\theta|\lambda}$ , assuming that  $\mathbb{P}_\lambda$  is known. A naive approach to compute the cut distribution would then be to generate samples from  $\mathbb{P}_{\theta|\lambda}$  for a large set of samples  $\lambda$  drawn from  $\mathbb{P}_\lambda$ . Unfortunately, this sampling scheme is computationally expensive and does not leverage the fact that, under some regularity conditions, the conditional distribution of  $\theta$  given  $\lambda$  may provide some information about  $\theta$  given  $\lambda'$  if  $\lambda$  and  $\lambda'$  are close to each other. Instead, we present another approach that directly computes the probability distribution of the functional parameter  $\theta(\lambda)$ . This nonparametric approach represents each component of  $\theta(\lambda)$  as a trajectory of a Gaussian process, which is inspired by the work of [6] in another calibration context. In the present paper, the functional approach will be presented in the case where the output of the downstream model is expressed as a linear function of  $\theta$ . This assumption makes it feasible to derive analytically the posterior predictive distribution of  $\theta$  conditional on any realization of  $\lambda$  drawn from  $\mathbb{P}_\lambda$ . The performance of the approach will be illustrated numerically on several academic examples.

The paper is organized into five parts presenting the statistical framework of the functional approach, while its implementation on the two ALCYONE solver models is deferred to future work. Section 2 introduces Bayesian calibration of two chained numerical models, including a brief review of the seminal work of Kennedy and O’Hagan and a presentation of the cut posterior distribution. Section 3 deals with several possible methods for conditional density estimation. In Section 4, the functional approach called GP-LinCC for Gaussian process and linear-based Conditional Calibration is developed. Its numerical performance will be demonstrated in Section 5. Section 6 ends the paper with some conclusions and perspectives.

## 2 Bayesian calibration of two chained numerical models

### 2.1 The full posterior versus the cut posterior

We deal with a computer model  $y$  that is supposed to be representative of a physical system of interest  $r$ . The latter yields a scalar quantity of interest  $r(x)$ , where  $x \in \mathcal{X} \subset \mathbb{R}^d$  denotes an input vector composed of control variables such as boundary and initial conditions. Let us assume that the computer model is written as the composition of two submodels. Then

$$y_{\theta,\lambda}(x) := y_\theta^2(y_\lambda^1(x)) \quad (1)$$

with the input variables of the downstream model being the outputs of the upstream model. The computer model often needs to be parameterized by calibration or tuning parameters, which may have no direct experimental counterpart [27, 18]. In Eq. (1),  $\theta$  and  $\lambda$  refer to the parameters of the downstream and upstream models respectively.

Being uncertain, these parameters are usually estimated to obtain the best agreement between the computer model and the physical system. This procedure is known as model calibration and relies on the availability of experimental observations of  $r(x)$ . For  $1 \leq i \leq n$ , an experimental observation  $z_i$  at a specific input location  $x_i$  is in fact related to  $r(x_i)$  by the equation

$$z_i = r(x_i) + \epsilon_{z_i} \quad (2)$$

where  $\epsilon_{z_i}$  is the realization of a zero-mean Gaussian distribution representing the experimental uncertainty. Then, the computer model replaces  $r(x)$  in Eq. (2), up to a discrepancy function  $b$  [22]:

$$z_i = y_{\theta,\lambda}(x_i) + b(x_i) + \epsilon_{z_i}, \quad 1 \leq i \leq n, \quad (3)$$

The function  $b(x)$ , called model discrepancy, is originally presented by Kennedy and O’Hagan in [22] to represent the gap between the numerical model  $y_{\theta,\lambda}(x)$  and the physical system  $r(x)$  when the model is run at the optimal (but unknown) value  $(\theta, \lambda)$  of the parameters<sup>1</sup>. If  $b(x)$  is judged negligible compared to the experimental uncertainty [13], the following simplified equation can be chosen instead:

$$z_i = y_{\theta,\lambda}(x_i) + \epsilon_{z_i}. \quad (4)$$

Assuming that the standard deviation of  $\epsilon_{z_i}$ , denoted  $\sigma_{\epsilon_{z_i}}$ , is known, the joint posterior distribution of  $(\theta, \lambda)$  based on Eq. (4) is obtained via Bayes’ theorem as

$$\pi(\theta, \lambda|z) \propto \mathcal{L}(z|\theta, \lambda) \pi(\theta, \lambda), \quad (5)$$

where  $\pi(\theta, \lambda)$  is the prior density that quantifies the uncertainty of  $(\theta, \lambda)$  before collecting the data  $z$ ,  $\mathcal{L}(z|\theta, \lambda)$  is the likelihood of the data  $z$  conditional on the pair  $(\theta, \lambda)$  and  $\pi(\theta, \lambda|z)$  is the posterior density that quantifies the residual uncertainty of  $(\theta, \lambda)$  conditional on  $z$ . Note that the same symbol  $\pi$  is used on both sides to denote, respectively, the prior and posterior densities. This notation avoids introducing  $\pi_{\text{prior}}(\cdot)$  and  $\pi_{\text{post}}(\cdot)$  and does not imply that the two densities correspond to the same function.

Eq. (4) relies on experimental data from the last stage of the simulation chain. When additional data informing the parameter  $\lambda$  of the thermal model are available, cut-off models can be used. They explicitly partition the different sources of information contributing to the identification of  $(\theta, \lambda)$  [25, 36, 21]. Inspired by the work of Plummer [36], Figure 2 presents a cut-off model for the chaining in Eq. (1) where the direct measurements  $w$  (a realization of some random variable  $W$ ) bring information about  $\lambda$  through comparisons with the outputs of the upstream model:

$$w_j = y_{\lambda}^1(x_j) + \epsilon_{w_j}, \quad 1 \leq j \leq n_1, \quad (6)$$

where  $\epsilon_{w_j}$  is still the realization of a zero-mean Gaussian distribution. In this figure, the graph is partitioned by a cut between the two models, preventing the data  $z$  (a

---

<sup>1</sup>Optimal in the sense that the model run with  $(\theta, \lambda)$  yields the best possible predictive accuracy. Note that this optimal value may differ from the true parameter [22, 43].

realization of  $Z$ ) from influencing the estimation of  $\lambda$ . On the left-hand side, the posterior distribution of  $\lambda$  is computed independently of the data  $z$ . In other words, the resulting estimate relies exclusively on the observation  $w$  of  $W$ , despite the additional information provided by  $Z$ .

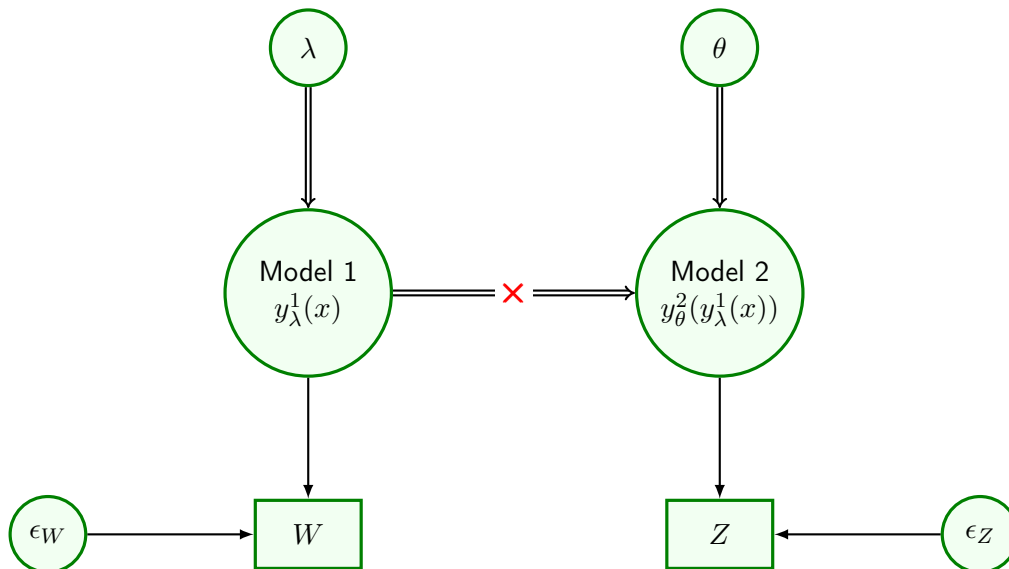


Figure 2: Graphical representation of a cut-off model for two chained models. Single and double arrows, respectively, denote stochastic and deterministic functional dependencies. Rectangular nodes represent observed data; the red cross indicates that information from  $Z$  does not back-propagate to  $\lambda$ .

Then, we can write the probability distribution of the parameters  $(\theta, \lambda)$  conditional on the complete data  $(W = w, Z = z)$  as in Eq. (5) of [21]:

$$\pi_{\text{cut}}(\theta, \lambda | w, z) = \pi(\theta | \lambda, z) \pi(\lambda | w), \quad (7)$$

where

$$\pi(\lambda | w) \propto \mathcal{L}(w | \lambda) \pi(\lambda) \quad (8)$$

is the posterior distribution of  $\lambda$  with respect only to the data  $w$  of the upstream model, and  $\pi(\theta | \lambda, z)$  is the posterior distribution of  $\theta$  conditional on  $\lambda$  with respect to the data  $z$  of the downstream model. The density  $\pi_{\text{cut}}(\theta, \lambda | w, z)$ , called the cut distribution in [36], does not coincide with the regular joint posterior density, denoted by  $\pi_{\text{full}}(\theta, \lambda | w, z)$ , which is written as:

$$\pi_{\text{full}}(\theta, \lambda | w, z) = \pi(\theta | \lambda, z) \pi(\lambda | w, z). \quad (9)$$

It turns out that these two distributions are linked by the following equations:

$$\frac{\pi_{\text{full}}(\theta, \lambda | w, z)}{\pi_{\text{cut}}(\theta, \lambda | w, z)} = \frac{\pi(\lambda | w, z)}{\pi(\lambda | w)} = \frac{\pi(z | \lambda)}{\pi(z | w)}. \quad (10)$$

## 2.2 Illustrative numerical example for a simple calibration problem

Let us consider the simple analytical example below, inspired by DeCarlo et al. [14]. For  $1 \leq j \leq n_1$  and  $1 \leq i \leq n = n_2$ ,

$$\begin{cases} w_j = \lambda + \epsilon_{w_j} & ; \quad \epsilon_{w_j} \sim \mathcal{N}(0, \sigma_w^2), \\ z_i = x_i \lambda + \theta + \epsilon_{z_i} & ; \quad \epsilon_{z_i} \sim \mathcal{N}(0, \sigma_z^2), \end{cases} \quad (11)$$

with  $\sigma_z^2 = 0.15$  and  $\sigma_w^2 = 0.15$ . Eq. (11) can be rewritten as

$$y = \begin{pmatrix} w \\ z \end{pmatrix} = A_x \begin{pmatrix} \lambda \\ \theta \end{pmatrix} + \begin{pmatrix} \epsilon_w \\ \epsilon_z \end{pmatrix}, \quad (12)$$

with

$$A_x = \begin{pmatrix} \mathbf{1}_{n_1} & \mathbf{0}_{n_1} \\ x & \mathbf{1}_{n_2} \end{pmatrix} ; \quad x = (x_1, \dots, x_{n_2})^t \quad (13)$$

and

$$\begin{pmatrix} \epsilon_w \\ \epsilon_z \end{pmatrix} \sim \mathcal{N}_{n_1+n_2} \left( 0, \Sigma_\sigma := \begin{pmatrix} \sigma_w^2 I_{n_1} & 0 \\ 0 & \sigma_z^2 I_{n_2} \end{pmatrix} \right). \quad (14)$$

The impact of two different prior distributions on  $\pi_{\text{full}}$  and  $\pi_{\text{cut}}$  will be assessed:

1. An informative Gaussian prior on  $\xi := (\lambda, \theta)^\top$  given by

$$\xi \sim \mathcal{N} \left( \xi_0 := \begin{pmatrix} \lambda_0 \\ \theta_0 \end{pmatrix}, \Sigma_0 := \begin{pmatrix} \sigma_{\lambda_0}^2 & 0 \\ 0 & \sigma_{\theta_0}^2 \end{pmatrix} \right). \quad (15)$$

2. A Jeffreys prior on  $\xi$ , i.e.,

$$\pi(\xi) \propto 1. \quad (16)$$

The expressions of both the full and cut posterior distributions can be explicitly derived, as well as the KL divergence between the two (see Appendix B). The following results have been established:

1. With Gaussian prior:

$$\text{KL}(\pi(\lambda|w, z) \parallel \pi(\lambda|w)) = 0 \iff \forall i, x_i = 0. \quad (17)$$

2. With Jeffreys prior:

$$\text{KL}(\pi(\lambda|w, z) \parallel \pi(\lambda|w)) = 0 \iff \forall i, x_i = c \in \mathbb{R}. \quad (18)$$

Eq. (17) follows directly from the fact that the two models are no longer linked to one another. Nonidentifiability means that multiple pairs  $(\theta, \lambda)$  can yield identical predictions for the downstream model, as occurs when all  $x_i$  are equal to a constant  $c$ . In this setting, Eq. (18) shows that nothing is gained by computing  $\pi_{\text{full}}$  instead of  $\pi_{\text{cut}}$  when a Jeffreys prior is used. When a Gaussian prior is used instead, Eq. (17) states that

the KL divergence is nonzero. To illustrate this, we generated the data  $w$  and  $z$  with sample sizes  $n_1 = n_2 = 15$ , the true parameter values  $\theta = 0.9$ ,  $\lambda = 1.2$ ,  $c = 5$ , and variances  $\sigma_z^2 = 0.15$  and  $\sigma_w^2 = 0.15$ . Figure 3 displays the histograms of  $\pi_{\text{cut}}(\theta, \lambda|w, z)$  and  $\pi_{\text{full}}(\theta, \lambda|w, z)$  together with a scatter plot of the 2-D posterior samples. Although the gap between the two distributions is moderate,  $\pi_{\text{full}}$  outperforms  $\pi_{\text{cut}}$  because the chosen prior density for  $\theta$  agrees sufficiently well with the data  $z$ . However, this behavior is not systematic, and the full posterior distribution might be less accurate than the cut distribution, depending on the interaction between the value of  $c$  and the shape of the prior, as shown in [25, 21].

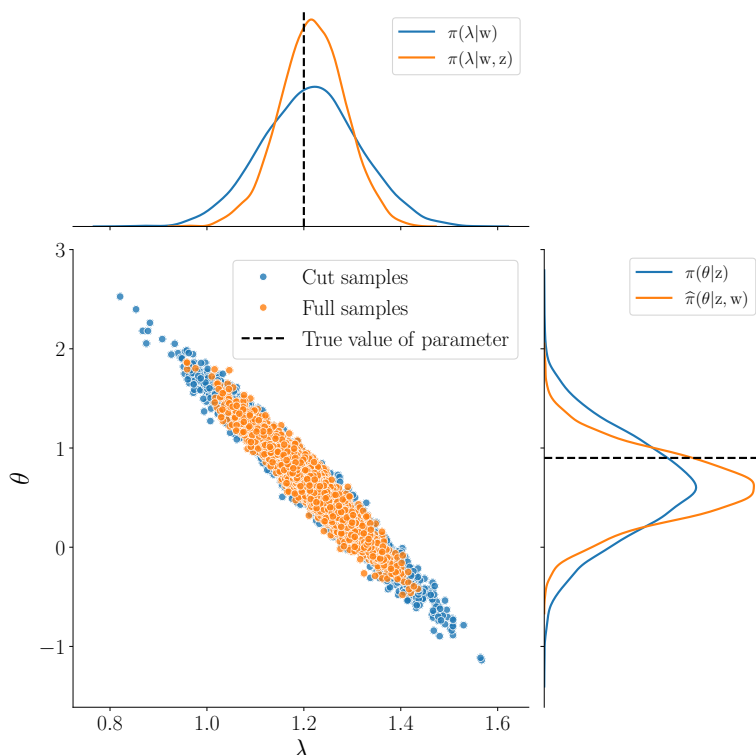


Figure 3: Comparison of the joint distribution of  $(\theta, \lambda)$  obtained from the cut posterior  $\pi_{\text{cut}}(\theta, \lambda|w, z)$  (red) and the full posterior  $\pi_{\text{full}}(\theta, \lambda|w, z)$  (blue) under the Gaussian prior  $\pi(\theta, \lambda)$  of Eq. (15) with  $\lambda_0 = 1$ ,  $\theta_0 = 0.7$  and  $\sigma_{\lambda_0}^2 = 1$ ,  $\sigma_{\theta_0}^2 = 0.2$ . The notation  $\hat{\pi}(\cdot|v)$  refers to the kernel density estimator of  $\pi(\cdot|v)$ .

We now turn to the identifiable setting, that is, when  $x_i$  varies. A more significant gap between  $\pi_{\text{full}}$  and  $\pi_{\text{cut}}$  appears, regardless of the prior type. Figure 4 shows the posterior distributions when the Jeffreys prior is used and  $z$  is simulated with

$$x_i \sim \mathcal{U}[-6, 6], \quad 1 \leq i \leq n_2 = 15 \quad (19)$$

and with the same values as before for  $\theta$ ,  $\lambda$ ,  $\sigma_z^2$ , and  $\sigma_w^2$ . Since the data  $z$  now provide

additional information about  $\lambda$ , using  $\pi_{\text{full}}$  will always yield a significantly more precise estimate of  $\lambda$ . We can also see that the posterior covariance between  $\lambda$  and  $\theta$  is strongly modified.

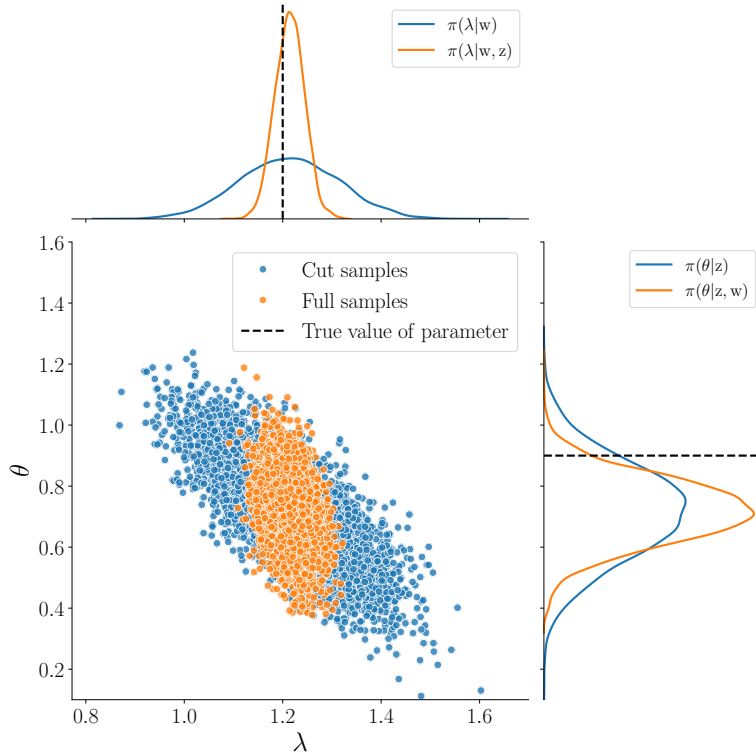


Figure 4: Comparison of the joint distribution of  $(\theta, \lambda)$  obtained from the cut posterior  $\pi_{\text{cut}}(\theta, \lambda|w, z)$  (red) and from the full posterior  $\pi_{\text{full}}(\theta, \lambda|w, z)$  (blue) under a Jeffreys prior  $\pi(\theta, \lambda)$  of Eq. (16).

In these well-specified synthetic examples, i.e., where the data-generating process coincides with the model used for inference, we have illustrated the impact of downstream model identifiability on the shape of  $\pi_{\text{full}}$  and  $\pi_{\text{cut}}$ .

Under model misspecification, even when the downstream model is identifiable, Section 3 of [21] shows that the full posterior may yield suboptimal predictive performance, whereas modular strategies such as the cut distribution can lead to better-calibrated predictions. This situation typically arises when a model-discrepancy term  $b(x)$  in Eq. (3) exists between the outputs of the chained models and the corresponding observations but is omitted in the Bayesian calibration process. Introducing  $b(x)$  would substantially increase inference complexity and may implicitly reveal structural limitations of the numerical model, which partly explains its limited adoption in engineering practice. In fuel-performance simulations where current calibration practices do not incorporate  $b(x)$ , the cut distribution is therefore particularly appropriate. A final argument in fa-

vor of the cut posterior is that the experimental data  $z$  associated with the fission-gas behavior model provide much weaker information about  $\lambda$  than the thermal-model data  $w$ . The contribution of  $z$  may thus be counterproductive, making the full posterior less accurate than the cut posterior for estimating  $\lambda$ .

In the rest of the paper, we develop a new method, called GP–LinCC (Gaussian process and linear-based Conditional Calibration), to compute the cut posterior distribution when the posterior density  $\pi(\lambda|w)$  is known. This reduces to estimating the conditional posterior density  $\pi(\theta|z, \lambda)$ . The next section highlights the limitations of existing approaches for this task and introduces the key components of GP–LinCC.

### 3 Methods for conditional density estimation

#### 3.1 Nonparametric approach via a kernel density estimation (KDE)

An estimate of the conditional density  $\pi(\theta|\lambda, z)$  can be defined as:

$$\hat{\pi}(\theta|\lambda, z) = \frac{\hat{\pi}_{\text{cut}}(\theta, \lambda|w, z)}{\pi(\lambda|w)} \quad (20)$$

where  $\hat{\pi}_{\text{cut}}$  denotes a KDE estimate [24, 34] of  $\pi_{\text{cut}}(\theta, \lambda|w, z)$ . While in standard conditional density estimation the denominator in Eq. (20) is also approximated using KDE [8],  $\pi(\lambda|w)$  is known in our setting, which simplifies the ratio estimation. The numerator is approximated from a large number of samples  $\{\theta_i, \lambda_i\}_{i=1}^N$  drawn from  $\pi_{\text{cut}}(\theta, \lambda|w, z)$ . These samples can be generated using a Gibbs sampler from the class of Markov chain Monte Carlo (MCMC) algorithms [37]. Starting from an initial value  $\lambda_0$ , the algorithm proceeds as follows: for  $1 \leq i \leq N$ ,

$$\theta_i \sim \pi(\theta|\lambda_{i-1}, z) \propto \pi_{\text{full}}(\theta, \lambda_{i-1}|w, z), \quad (21)$$

$$\lambda_i \sim \pi(\lambda|\theta_i, z) \propto \frac{\pi_{\text{full}}(\theta_i, \lambda|w, z)}{\pi(z|\lambda)}. \quad (22)$$

$N$  should be large enough to allow convergence of this sampling scheme towards the cut distribution. Unfortunately, in the general case, the marginal likelihood in the denominator of Eq. (22), called the *feedback* term in [21], has no closed form:

$$\pi(z|\lambda) = \int_{\mathcal{T}} \mathcal{L}(z|\theta, \lambda) \pi(\theta|\lambda) d\theta. \quad (23)$$

Unless a complex approximation of the feedback term is used [26], the above sampling scheme is infeasible. Instead, a simple approach implemented in Jacob et al. [20] may be to sample, for any realization  $\lambda_i$  drawn from  $\pi(\lambda|w)$ , the associated conditional posterior distribution: for  $1 \leq i \leq N$ ,

$$\lambda_i \sim \pi(\lambda|w), \quad (24)$$

$$\theta_i \sim \pi(\theta|\lambda_i, z). \quad (25)$$

If the conditional density in Eq. (25) is known only up to a constant, drawing one sample  $\theta_i$  requires a specific MCMC algorithm depending on  $\lambda_i$ . This sampling scheme thus involves as many Markov chains as the number of realizations  $\lambda_i$  drawn from  $\pi(\lambda|w)$ , and the convergence of each Markov chain must be diagnosed carefully to ensure accurate sampling of the cut distribution. Moreover, if the computer model is even moderately time-consuming, the total number of generated samples  $(\lambda_i, \theta_i)$  may be insufficient to construct a reliable KDE. This motivates the moment-based method presented below, where a regression model fits the conditional density  $\pi(\theta|\lambda, z)$  as a function of  $\lambda$ .

### 3.2 Moment-based estimation method

Let us consider a numerical design, denoted by  $D_m$ , consisting of  $m$  realizations  $\lambda_j \sim \pi(\lambda|w)$  generated by Latin hypercube sampling [32]. Given a set of posterior samples  $(\theta_j^{(i)})_{i=1}^N$  associated with each  $\lambda_j$ , the posterior expectation and the variance matrix of the conditional distribution in Eq. (25) can be estimated by

$$\bar{\theta}(\lambda_j) := \mathbb{E}(\theta|\lambda_j, z) \approx \frac{1}{N} \sum_{i=1}^N \theta_j^{(i)}, \quad (26)$$

$$\text{cov}(\theta|\lambda_j, z) \approx \frac{1}{N} \sum_{i=1}^N (\theta_j^{(i)} - \bar{\theta}(\lambda_j))(\theta_j^{(i)} - \bar{\theta}(\lambda_j))^t. \quad (27)$$

Then, a Gaussian process (GP) emulator (see Section 3.3.1 for a brief introduction) can be used to interpolate the first two moments (26) and (27), enabling predictions of the mean and variance of  $\mathbb{P}_{\theta|\lambda}$  for any realization  $\lambda^* \notin D_m$ . The main problem lies in preserving the positive semidefinite property of the variance matrix. The GP can be fitted on the log variance if  $\theta$  is a scalar parameter ( $p = 1$ ). For  $p > 1$ , the solution proposed in [16] consists of fitting a GP on each Cholesky factor, then using the inverse Cholesky decomposition to obtain a matrix ensuring the positive semi-definite property. However, this method is rather costly when  $p$  is large and does not provide any uncertainty of the predicted matrix.

In the rest of the paper, the downstream model is approximated by a linear function of  $\theta$  conditional on  $\lambda$  (see Section 3.3.2). This assumption is appropriate when the model output can be reasonably approximated by a linear function of  $\theta$ , as in the case of the fission-gas behavior model. This implies that Eq. (25) no longer requires MCMC, although a large number of samples  $(\lambda_i, \theta_i)$  is still needed. In the linear framework, the moment-based method becomes easier to implement because the posterior of  $\theta$  conditional on  $\lambda$  can be computed explicitly as a Gaussian distribution provided the prior density  $\pi(\theta|\lambda)$  is Gaussian. However, the difficulty of interpolating variance matrices remains. In the GP-LinCC method presented in the next section, we adopt a Bayesian approach by fitting a GP emulator embedded as a prior distribution on  $\theta(\lambda)$ .

### 3.3 Proposed solution: method based on GP-prior and linear assumption (GP–LinCC method)

#### 3.3.1 Gaussian Process prior

Gaussian processes (GPs) are widely used to emulate computationally expensive black-box computer models [38]. A GP defines a prior over the response function of such models, fully characterized by a mean function and a covariance kernel. Conditioned on observed data, the resulting posterior GP yields a Gaussian predictive distribution for the model output at any input location, with closed-form expressions for the predictive mean and covariance matrix [10] (see Appendix A.2). In nuclear computational modeling, GPs have been used to address inverse uncertainty quantification [12], to identify penalizing configurations for safety studies [31], and for various other applications. In a context close to that of this paper, GPs were used to emulate a chain of two numerical models for calibration purposes [29]. Still in the context of model calibration, a GP has been used in [6] to capture the functional relationship between a calibration parameter and some input control variables. In our framework, inspired by the latter reference, we model the relationship between  $\theta$  and  $\lambda$  by assuming that each component of  $\theta(\lambda) \in \mathbb{R}^p$  follows an independent GP a priori, such that

$$\theta_u(\lambda) \stackrel{\text{indep.}}{\sim} \mathcal{GP}(m_{\beta_u}(\lambda), \sigma_u^2 K_{\psi_u}(\lambda, \lambda')), \quad 1 \leq u \leq p, \quad (28)$$

where  $m_{\beta_u}(\lambda)$  is the mean function (also called trend) of the  $u$ th GP. A constant  $m_{\beta_u}(\lambda) = \beta_u$  or a degree-one polynomial trend is commonly used in practice.

For simplicity, we assume in the sequel that the prior mean is constant and equal to  $\beta_u$ . The covariance function  $\sigma_u^2 K_{\psi_u}(\lambda, \lambda')$  controls both the regularity and the scale of the GP trajectories. It encodes the dependence structure of the  $u$ th GP and must be positive semidefinite. When  $\theta_u(\lambda)$  is assumed to be highly smooth, the Matérn 5/2 covariance function is among the most commonly used choices, as recommended in particular in [17]. It is defined as

$$\sigma_u^2 K_{\psi_u}(\lambda, \lambda') = \sigma_u^2 \left( 1 + \sqrt{5} \frac{|\lambda - \lambda'|}{\psi_u} + \frac{5}{3} \left( \frac{|\lambda - \lambda'|}{\psi_u} \right)^2 \right) \exp\left( -\sqrt{5} \frac{|\lambda - \lambda'|}{\psi_u} \right). \quad (29)$$

In the multidimensional case (i.e.,  $\lambda \in \mathbb{R}^q$  with  $q \geq 1$ ), either an isotropic or a separable (tensor-product) Matérn 5/2 covariance function may be employed (see, for example, [2]).

#### 3.3.2 Linear approximation

The advantage of a linear framework is that the posterior distribution of  $\theta$  conditional on  $\lambda$  can be derived analytically. We assume that, for any  $\lambda$ , the output of the numerical model  $y_{\theta(\lambda), \lambda}(x_i)$  can be written, or approximated, as a linear function of  $\theta(\lambda)$ . Thus, for  $1 \leq i \leq n$ , Eq. (4) can be rewritten as

$$z_i = g_{\lambda,0}(x_i) + g_{\lambda,1}(x_i)^t \theta(\lambda) + \epsilon_{i,\lambda}, \quad \epsilon_{i,\lambda} \sim \mathcal{N}(0, \sigma_{\epsilon_i}^2 + \delta_{\lambda,i}^2), \quad (30)$$

where  $\delta_{\lambda,i}^2$  is a scale parameter capturing the discrepancy between the model output and its linear approximation. In practice, the regression coefficients are collected in the vector

$$g_{\lambda}(x_i) := (g_{\lambda,0}(x_i), g_{\lambda,1}(x_i))^t \in \mathbb{R}^{p+1}. \quad (31)$$

These coefficients must be estimated at fixed  $(\lambda, x_i)$ , either by performing a local linearization at a specific  $\theta(\lambda) = \tilde{\theta}(\lambda)$  or by using a variational linear approximation over  $\mathcal{T} \ni \theta$ . We adopt the latter approach, as advocated in a recent paper addressing the identifiability of inverse problem solutions [5]. A linear regression model is then fitted for each pair  $(\lambda_j, x_i)$  using a set of  $n_{\text{sim}}$  training samples defined as

$$\Theta^{(j)} := \{\theta_1^{(j)}, \dots, \theta_{n_{\text{sim}}}^{(j)}\} \subset \mathcal{T}^{n_{\text{sim}}}. \quad (32)$$

A total of  $m \times n \times n_{\text{sim}}$  simulations are therefore required to fit the  $m \times n$  linear models.

## 4 The GP-LinCC method

Building on the linear framework introduced previously, Section 4.1 establishes that combining the Gaussian prior in Eq. (28) with a Gaussian likelihood yields a Gaussian posterior distribution. Section 4.2 further shows that this structure leads to a Gaussian predictive distribution for  $\theta$  conditional on any  $\lambda$  with non-zero probability under  $\pi(\lambda|w)$ .

The practical implementation of the GP-LinCC method needs the following set of simulations of the chain model:

$$\cup_{j=1}^m \cup_{k=1}^{n_{\text{sim}}} \{y_{\theta_k^{(j)}, \lambda_j}(x_i)\}_{i=1, \dots, n}. \quad (33)$$

These simulations make it possible to estimate all the vectors  $g_{\lambda_j}(x_i)$  for  $1 \leq i \leq n$  and  $1 \leq j \leq m$ , and thus to fit the  $m \times n$  linear models required by the approach.

### 4.1 Posterior inference

We apply Eq. (30) to the  $m$  realizations  $\lambda_j$  to learn the relation between  $\theta$  and  $\lambda$ . We can then write  $m$  equations involving the experimental data  $z = (z_1, \dots, z_n)^t \in \mathbb{R}^n$ :

$$z = g_{\lambda_j}(x) \theta(\lambda_j) + \epsilon_{\lambda_j}, \quad 1 \leq j \leq m, \quad (34)$$

where

$$g_{\lambda_j}(x) := (g_{\lambda_j}(x_1)^t, \dots, g_{\lambda_j}(x_n)^t)^t \in \mathbb{R}^{n \times p}, \quad \epsilon_{\lambda_j} := (\epsilon_{1, \lambda_j}, \dots, \epsilon_{n, \lambda_j})^t.$$

We assume  $g_{\lambda_j,0}(x_i) = 0$ . If  $g_{\lambda_j,0}(x_i)$  is non-zero, this term can be subtracted from the left-hand side of Eq. (34), as illustrated in the numerical examples of Section 5. Note that the same experimental vector  $z$  appears in all  $m$  equations, as it is compared to the model output evaluated at each  $\lambda_j$ . Accordingly,  $z$  is replicated  $m$  times in the matrix formulation below, which gathers these  $m$  equations into a single matrix expression:

$$(z, \dots, z) = (g_{\lambda_1}(x) \theta(\lambda_1), \dots, g_{\lambda_m}(x) \theta(\lambda_m)) + (\epsilon_{\lambda_1}, \dots, \epsilon_{\lambda_m}). \quad (35)$$

Let  $\mathbf{z} := (z, \dots, z) \in \mathbb{R}^{n \times m}$  be the matrix of the  $m$  copies of  $z$ , and let the associated macro-parameter matrix be  $\Theta_m := (\theta(\lambda_1), \dots, \theta(\lambda_m))^t \in \mathbb{R}^{m \times p}$ . Each  $\theta(\lambda_j)$  follows a multivariate normal distribution arising from Eq. (28). One way to infer  $\Theta_m$  is to work with its vectorized form, denoted  $\vec{\Theta}_m := \text{vec}(\Theta_m)$  [4] (see Appendix A.1), whose prior density is written as:

$$\pi(\vec{\Theta}_m | \phi) \propto |\mathbf{C}_\phi|^{-1/2} \exp \left\{ -\frac{1}{2} (\vec{\Theta}_m - \vec{M}_\beta)^t \mathbf{C}_\phi^{-1} (\vec{\Theta}_m - \vec{M}_\beta) \right\}, \quad (36)$$

where

$$\vec{M}_\beta = (m_{\beta_1}(\lambda_1), \dots, m_{\beta_p}(\lambda_1), \dots, m_{\beta_1}(\lambda_m), \dots, m_{\beta_p}(\lambda_m))^t \in \mathbb{R}^{pm}, \quad (37)$$

and

$$\mathbf{C}_\phi = \{\text{cov}(\theta(\lambda_j), \theta(\lambda_{j'}))\}_{j,j'=1}^m, \quad \text{cov}(\theta(\lambda_j), \theta(\lambda_{j'})) = \text{diag}\{\sigma_l^2 K_{\psi_l}(\lambda_j, \lambda_{j'})\}_{l=1}^p, \quad (38)$$

and

$$\phi := \{(\beta_l, \sigma_l^2, \psi_l)\}_{l=1}^p. \quad (39)$$

Although the parameters  $\beta_l$  enter only through the prior mean  $\vec{M}_\beta$ , we collect them together with the covariance hyperparameters  $(\sigma_l^2, \psi_l)$  into the vector  $\phi$  for notational convenience.

Let  $\vec{\mathbf{z}} := \text{vec}(\mathbf{z})$  denote the vectorized form of the matrix  $\mathbf{z} = (z, \dots, z)$ , and let  $\vec{\epsilon}$  denote the vectorized form of  $(\epsilon_{\lambda_1}, \dots, \epsilon_{\lambda_m})$ . One can then rewrite Eq. (35) in its vectorized form:

$$\vec{\mathbf{z}} = \begin{pmatrix} g_{\lambda_1}(x) \theta(\lambda_1) \\ \vdots \\ g_{\lambda_m}(x) \theta(\lambda_m) \end{pmatrix} + \vec{\epsilon} \quad (40)$$

$$= G \vec{\Theta}_m + \vec{\epsilon}, \quad \vec{\epsilon} \sim \mathcal{N}(0, \Sigma_{\vec{\epsilon}}),$$

where

$$G = \text{diag}(g_{\lambda_1}(x), \dots, g_{\lambda_m}(x)) \in \mathbb{R}^{nm \times pm}, \quad (41)$$

$$\Sigma_{\vec{\epsilon}} = \text{diag}(\Sigma_{\epsilon_{\lambda_1}}, \dots, \Sigma_{\epsilon_{\lambda_m}}) \in \mathbb{R}^{nm \times nm}, \quad (42)$$

$$\Sigma_{\epsilon_{\lambda_j}} = \text{diag}(\sigma_{\epsilon_1}^2 + \delta_{\lambda_j,1}^2, \dots, \sigma_{\epsilon_n}^2 + \delta_{\lambda_j,n}^2), \quad 1 \leq j \leq m. \quad (43)$$

Assume that the covariance matrix  $\Sigma_{\vec{\epsilon}}$  is symmetric positive definite. The likelihood of  $\vec{\mathbf{z}}$  conditionally on  $\vec{\Theta}_m$  is given by:

$$\mathcal{L}(\vec{\mathbf{z}} | \vec{\Theta}_m) \propto \exp \left\{ -\frac{1}{2} (\vec{\mathbf{z}} - G \vec{\Theta}_m)^t \Sigma_{\vec{\epsilon}}^{-1} (\vec{\mathbf{z}} - G \vec{\Theta}_m) \right\}. \quad (44)$$

Finally, by Bayes' formula:

$$\pi(\vec{\Theta}_m | \vec{\mathbf{z}}, \phi) \propto \mathcal{L}(\vec{\mathbf{z}} | \vec{\Theta}_m) \pi(\vec{\Theta}_m | \phi). \quad (45)$$

**Theorem 1.** Assume that the prior covariance matrix  $\mathbf{C}_\phi$  is symmetric positive definite. We can define

$$\Delta^{-1} := G^t \Sigma_\epsilon^{-1} G = \text{diag}\left(g_{\lambda_1}(x)^t \Sigma_{\epsilon_{\lambda_1}}^{-1} g_{\lambda_1}(x), \dots, g_{\lambda_m}(x)^t \Sigma_{\epsilon_{\lambda_m}}^{-1} g_{\lambda_m}(x)\right). \quad (46)$$

The posterior distribution  $\pi(\vec{\Theta}_m | \vec{\mathbf{z}}, \phi)$  is multivariate normal with mean  $\mu_\phi$  and covariance matrix  $\Sigma_\phi$  given by:

$$\mu_\phi = \Sigma_\phi (\mathbf{C}_\phi^{-1} \vec{M}_\beta + G^t \Sigma_\epsilon^{-1} \vec{\mathbf{z}}) \in \mathbb{R}^{pm}, \quad (47)$$

$$\Sigma_\phi = (\Delta^{-1} + \mathbf{C}_\phi^{-1})^{-1} \in \mathbb{R}^{pm \times pm}. \quad (48)$$

See Appendix C.1 for the proof.

## 4.2 Predictive distribution of $\theta(\lambda)$

For any new set of realizations  $\lambda^* = (\lambda_1^*, \dots, \lambda_k^*)^t$  drawn from  $\pi(\lambda | w)$ , the predictive distribution of

$$\vec{\theta}(\lambda^*) := \text{vec}\left(\left(\theta(\lambda_1^*)^t, \dots, \theta(\lambda_k^*)^t\right)^t\right) \in \mathbb{R}^{pk} \quad (49)$$

is obtained by integrating the conditional Gaussian distribution  $\pi(\vec{\theta}(\lambda^*) | \vec{\Theta}_m, \phi)$

$$\pi_{\text{pred}}(\vec{\theta}(\lambda^*) | \vec{\mathbf{z}}, \phi) = \int_{\mathcal{T}^m} \pi(\vec{\theta}(\lambda^*) | \vec{\Theta}_m, \phi) \pi(\vec{\Theta}_m | \vec{\mathbf{z}}, \phi) d\vec{\Theta}_m. \quad (50)$$

**Theorem 2.** Let  $\lambda^{*'} = (\lambda_1^{*'}, \dots, \lambda_{k'}^{*'})^t$ . The predictive distribution  $\pi_{\text{pred}}(\vec{\theta}(\lambda^*) | \vec{\mathbf{z}}, \phi)$  is a multivariate normal distribution with mean  $\bar{\theta}_{\text{pred}}(\lambda^*)$  and cross-covariance matrix  $\Sigma_{\text{pred}}(\lambda^*, \lambda^{*'})$  given by

$$\bar{\theta}_{\text{pred}}(\lambda^*) = \vec{m}_\beta(\lambda^*) + \mathbf{C}(\lambda^*, D_m) \mathbf{C}_\phi^{-1} (\mu_\phi - \vec{M}_\beta) \in \mathbb{R}^{pk}, \quad (51)$$

and

$$\Sigma_{\text{pred}}(\lambda^*, \lambda^{*'}) = \Sigma_{\text{cond}}(\lambda^*, \lambda^{*'}) + \mathbf{C}(\lambda^*, D_m) \mathbf{C}_\phi^{-1} \Sigma_\phi \mathbf{C}_\phi^{-1} \mathbf{C}(D_m, \lambda^{*'}) \in \mathbb{R}^{pk \times pk'}, \quad (52)$$

where  $(\mu_\phi, \Sigma_\phi)$  are the posterior mean and covariance of  $\vec{\Theta}_m$  given in Theorem 1, and

$$\vec{m}_\beta(\lambda^*) = (m_{\beta_1}(\lambda_1^*), \dots, m_{\beta_p}(\lambda_1^*), \dots, m_{\beta_1}(\lambda_k^*), \dots, m_{\beta_p}(\lambda_k^*))^t \in \mathbb{R}^{pk}, \quad (53)$$

$$\mathbf{C}(\lambda^*, D_m) = \left[ \text{Cov}(\theta(\lambda_i^*), \theta(\lambda_j^*)) \right]_{1 \leq i \leq k, 1 \leq j \leq m} \in \mathbb{R}^{pk \times pm}, \quad (54)$$

$$\Sigma_{\text{cond}}(\lambda^*, \lambda^{*'}) = \mathbf{C}(\lambda^*, \lambda^{*'}) - \mathbf{C}(\lambda^*, D_m) \mathbf{C}_\phi^{-1} \mathbf{C}(D_m, \lambda^{*'}) \in \mathbb{R}^{pk \times pk'}. \quad (55)$$

Each entry of  $\mathbf{C}(\lambda^*, D_m)$  and  $\mathbf{C}(\lambda^*, \lambda^{*'})$  is a  $p \times p$  covariance block. See Appendix C.2 for the proof.

The expression of  $\bar{\theta}_{\text{pred}}(\lambda^*)$  follows the classical form of the conditional Gaussian process mean, except that the latent vector  $\vec{\Theta}_m$  is replaced by its posterior expectation  $\mu_\phi$ . An important advantage of GP-LinCC is that  $\bar{\theta}_{\text{pred}}(\lambda^*)$  provides a predictor of  $\theta(\lambda^*)$  without requiring the regression vectors  $g_{\lambda^*}(x_i)$  for  $1 \leq i \leq n$ . The predictive covariance  $\Sigma_{\text{pred}}(\lambda^*, \lambda^{*'})$  consists of two parts. The first component,  $\Sigma_{\text{cond}}(\lambda^*, \lambda^{*'})$ , is the usual GP interpolation variance, that is, the conditional covariance one would obtain as if the values of  $\vec{\Theta}_m$  were exactly known. It governs the transfer of uncertainty induced by Gaussian process interpolation across  $\lambda$ . The second term captures the posterior uncertainty on  $\vec{\Theta}_m$  and is governed by  $\Sigma_\phi$ . This term propagates the posterior uncertainty on the unknown parameters  $\vec{\Theta}_m$  to unseen values of  $\lambda$  through the covariance function. As  $m$  increases, only  $\Sigma_{\text{cond}}(\lambda^*, \lambda^*)$  is structurally reduced, because a richer design  $D_m$  limits the possible excursions of the GP between design points. By contrast, the second component of the predictive variance, driven by the uncertainty on  $\vec{\Theta}_m$  through  $\Sigma_\phi$ , is primarily decreased by enlarging the experimental sample size  $n$ .

For notational simplicity, we omit the superscript “ $\star$ ” in the predictive formulas and write  $\theta(\lambda)$  instead of  $\theta(\lambda^*)$  in the remainder of the paper.

All the previous formulas depend on the hyperparameters  $\phi$ , which are not known a priori. We estimate them using an empirical Bayes procedure based on marginal likelihood maximization [42]. This approach maximizes the marginal likelihood with respect to  $\phi$ , obtained by integrating out  $\vec{\Theta}_m$  from  $\mathcal{L}(\vec{z}|\vec{\Theta}_m)$ :

$$\hat{\phi} = \underset{\phi}{\operatorname{argmax}} \int_{\mathcal{T}^m} \mathcal{L}(\vec{z}|\vec{\Theta}_m) \pi(\vec{\Theta}_m|\phi) d\vec{\Theta}_m. \quad (56)$$

Appendix C.3 demonstrates that this integral has a closed form.

When the true functional parameter  $\theta_{\text{true}}(\lambda)$  is known, as in numerical experiments, parameter recovery can be evaluated using the predictive Integrated Mean-Squared Error (IMSE). It is defined as the posterior predictive squared loss relative to  $\theta_{\text{true}}(\lambda)$ , averaged with respect to  $\pi(\lambda|w)$ :

$$\text{IMSE} = \int_{\Lambda} \mathbb{E} \left[ (\theta(\lambda) - \theta_{\text{true}}(\lambda))^t (\theta(\lambda) - \theta_{\text{true}}(\lambda)) | \vec{z}, \phi \right] \pi(\lambda|w) d\lambda \quad (57)$$

where the inner expectation expands as

$$\mathbb{E} \left[ (\theta(\lambda) - \theta_{\text{true}}(\lambda))^t (\theta(\lambda) - \theta_{\text{true}}(\lambda)) | \vec{z}, \phi \right] = \sum_{u=1}^p \left( \Sigma_{\text{pred}}(\lambda, \lambda)_{u,u} + (\bar{\theta}_{\text{pred},u}(\lambda) - \theta_{\text{true},u}(\lambda))^2 \right). \quad (58)$$

In practice, the IMSE is estimated by Monte Carlo from a sample of size  $N_\lambda$ :

$$\text{IMSE} \approx \frac{1}{N_\lambda} \sum_{j=1}^{N_\lambda} \sum_{u=1}^p \left( \Sigma_{\text{pred}}(\lambda_j, \lambda_j)_{u,u} + (\bar{\theta}_{\text{pred},u}(\lambda_j) - \theta_{\text{true},u}(\lambda_j))^2 \right). \quad (59)$$

Then, the predictive cut distribution is defined as

$$\pi_{\text{cut,pred}}(\lambda, \theta|w, \vec{z}, \phi) := \pi(\lambda|w) \pi_{\text{pred}}(\theta(\lambda)|\vec{z}, \phi). \quad (60)$$

Eq. (60) mirrors the structure of the cut distribution in Eq. (7), with the density  $\pi(\theta|\lambda, z)$  replaced by the predictive density  $\pi_{\text{pred}}(\theta(\lambda)|\vec{z}, \phi)$ . In the synthetic examples presented in Section 5, we will examine the adequacy of this predictive approximation with respect to the target density  $\pi_{\text{cut}}(\lambda, \theta|w, z)$ . In these examples, the linear model  $g_\lambda(x_i)$  in Eq. (30) is known for all  $\lambda$ , which allows the explicit computation, for any  $\lambda$ , of the target conditional posterior distribution of  $\theta$  given  $\lambda$ . Under a Gaussian prior for  $\theta|\lambda$ ,

$$\theta(\lambda) \sim \mathcal{N}(m_0(\lambda), V_0(\lambda)), \quad (61)$$

we have

$$\theta|\lambda, z \sim \mathcal{N}(m_{\text{post}}(\lambda), V_{\text{post}}(\lambda)), \quad (62)$$

with

$$V_{\text{post}}(\lambda)^{-1} = V_0(\lambda)^{-1} + g_\lambda(x)^t \Sigma_{\epsilon_\lambda}^{-1} g_\lambda(x), \quad (63)$$

and

$$m_{\text{post}}(\lambda) = V_{\text{post}}(\lambda) \left( V_0(\lambda)^{-1} m_0(\lambda) + g_\lambda(x)^t \Sigma_{\epsilon_\lambda}^{-1} z \right). \quad (64)$$

Specifying instead the Jeffreys prior,

$$\pi(\theta|\lambda) \propto 1, \quad (65)$$

leads to

$$\theta|\lambda, z \sim \mathcal{N}_p \left( \hat{\theta}(\lambda), (g_\lambda(x)^t \Sigma_{\epsilon_\lambda}^{-1} g_\lambda(x))^{-1} \right), \quad (66)$$

where

$$\hat{\theta}(\lambda) = (g_\lambda(x)^t \Sigma_{\epsilon_\lambda}^{-1} g_\lambda(x))^{-1} g_\lambda(x)^t \Sigma_{\epsilon_\lambda}^{-1} z. \quad (67)$$

The discrepancy between the predictive and target conditional distributions may decrease once the design  $D_m$  becomes sufficiently informative. This occurs when  $m$  is large enough for the conditional covariance term  $\Sigma_{\text{cond}}(\lambda, \lambda)$  to remain uniformly small over the support of  $\lambda$ . In this regime, the interpolation uncertainty is largely suppressed, and the predictive variance induced by Eq. (52) is dominated by the propagation of posterior uncertainty through the term

$$\mathbf{C}(\lambda, D_m) \mathbf{C}_\phi^{-1} \Sigma_\phi \mathbf{C}_\phi^{-1} \mathbf{C}(D_m, \lambda), \quad (68)$$

leading to a closer agreement with the target posteriors. This second contribution does not structurally decrease with  $m$  for fixed hyperparameters. However, when  $\phi$  is estimated by empirical Bayes, the increase of  $m$  may induce an additional contraction of  $\Sigma_\phi$ . In that case, the predictive variance may become substantially smaller than the target posterior variance  $V_{\text{post}}(\lambda)$ , resulting in an over-concentrated predictive conditional distribution.

### 4.3 Predictive behavior of the chained model

For a given input configuration  $x_i$ , we define

$$r_i(\lambda) := g_\lambda(x_i)^t \theta(\lambda). \quad (69)$$

The predictive distribution of the output of the calibrated model is given by

$$r_i(\lambda) \mid \bar{\mathbf{z}}, \phi \sim \mathcal{N}(g_\lambda(x_i)^t \bar{\theta}_{\text{pred}}(\lambda), g_\lambda(x_i)^t \Sigma_{\text{pred}}(\lambda, \lambda) g_\lambda(x_i)). \quad (70)$$

Under a cross-validation scheme, Eq. (70) can be reformulated in a leave-one-out setting. For  $1 \leq i \leq n$ ,

$$r_i(\lambda) \mid \bar{\mathbf{z}}_{-i}, \phi \sim \mathcal{N}(g_\lambda(x_i)^t \bar{\theta}_{\text{pred},-i}(\lambda), g_\lambda(x_i)^t \Sigma_{\text{pred},-i}(\lambda, \lambda) g_\lambda(x_i)). \quad (71)$$

where  $\bar{\theta}_{\text{pred},-i}$  and  $\Sigma_{\text{pred},-i}$  are obtained from Theorem 2 by replacing  $\bar{\mathbf{z}}$  with  $\bar{\mathbf{z}}_{-i}$  (i.e.  $\bar{\mathbf{z}}$  with the  $i$ th observation removed). In the following, we consider the predictive random variable  $r_i$  obtained after marginalizing over  $\lambda \sim \pi(\lambda|w)$ . The predictive mean of  $r_i$ , obtained after marginalizing over  $\lambda \sim \pi(\lambda|w)$ , follows from the law of total expectation and is given by

$$\mathbb{E}[r_i \mid \bar{\mathbf{z}}_{-i}, \phi] = \mathbb{E}_{\lambda|w} \left[ g_\lambda(x_i)^t \bar{\theta}_{\text{pred},-i}(\lambda) \right]. \quad (72)$$

In order to quantify the total predictive uncertainty at  $x_i$ , the variance of  $r_i$  can then be decomposed with respect to  $\lambda$  using the law of total variance as

$$\mathbb{V}(r_i \mid \bar{\mathbf{z}}_{-i}, \phi) = \mathbb{E}_{\lambda|w} \left[ \mathbb{V}(r_i(\lambda) \mid \bar{\mathbf{z}}_{-i}, \phi) \right] + \mathbb{V}_{\lambda|w} \left( \mathbb{E}[r_i(\lambda) \mid \bar{\mathbf{z}}_{-i}, \phi] \right) \quad (73)$$

$$= \mathbb{E}_{\lambda|w} \left[ g_\lambda(x_i)^t \Sigma_{\text{pred},-i}(\lambda, \lambda) g_\lambda(x_i) \right] + \mathbb{V}_{\lambda|w} \left( g_\lambda(x_i)^t \bar{\theta}_{\text{pred},-i}(\lambda) \right). \quad (74)$$

The first term in Eq. (74) corresponds to the predictive variance of  $r_i(\lambda)$  conditionally on  $\lambda$ , averaged with respect to  $\pi(\lambda|w)$ . It therefore quantifies the residual posterior uncertainty on  $\theta(\lambda)$  after calibration, projected onto the scalar output  $r_i$ , for each fixed value of  $\lambda$ . The second term represents the variance, under  $\pi(\lambda|w)$ , of the conditional predictive mean  $g_\lambda(x_i)^t \bar{\theta}_{\text{pred},-i}(\lambda)$ , and thus measures the sensitivity of the calibrated prediction at  $x_i$  to the uncertainty on  $\lambda$ .

When the mean and variance of the conditional predictive distributions in Eq. (71) remain similar for different values of  $\lambda$ , and provided that the full posterior  $\pi(\lambda \mid \bar{\mathbf{z}}_{-i}, w)$  does not place substantial mass outside the support of  $\pi(\lambda|w)$ , the predictive distribution of  $r_i$  becomes weakly sensitive to the choice of the marginal distribution of  $\lambda$  and is therefore expected to be close to its full counterpart, in which the mean and variance in Eqs. (72)–(74) are taken with respect to  $\pi(\lambda \mid \bar{\mathbf{z}}_{-i}, w)$ . This situation is referred to as a *compensation effect*, and typically occurs when distinct pairs  $(\lambda_1, \theta(\lambda_1))$  and  $(\lambda_2, \theta(\lambda_2))$  lead to similar likelihood values, i.e. when the downstream model is non-identifiable.

To provide a more detailed characterization of such a potential compensation effect, it is therefore useful to examine how the predictive distribution varies with  $\lambda$ . If a

compensation effect occurs to some extent, then for typical values of  $\lambda_1 \neq \lambda_2$  drawn from  $\pi(\lambda|w)$ , the corresponding predictive densities

$$\pi(r_i(\lambda_1) | \vec{z}_{-i}, \phi) \quad \text{and} \quad \pi(r_i(\lambda_2) | \vec{z}_{-i}, \phi) \quad (75)$$

are expected to be similar. Such a compensation effect arises when the downstream model is non-identifiable to some extent, meaning that distinct pairs  $(\lambda_1, \theta(\lambda_1))$  and  $(\lambda_2, \theta(\lambda_2))$  lead to the same likelihood (see [9] for an in-depth discussion of nonidentifiability). Therefore, the predictive credibility interval of the random variable

$$r_i(\lambda_1) - r_i(\lambda_2) | \vec{z}_{-i}, \phi \quad (76)$$

is likely to contain 0. This random variable is Gaussian with mean

$$\mu_i(\lambda_1, \lambda_2) := \begin{pmatrix} g_{\lambda_1}(x_i) \\ -g_{\lambda_2}(x_i) \end{pmatrix}^t \begin{pmatrix} \bar{\theta}_{\text{pred},-i}(\lambda_1) \\ \theta_{\text{pred},-i}(\lambda_2) \end{pmatrix}, \quad (77)$$

and variance

$$\sigma_i^2(\lambda_1, \lambda_2) := \begin{pmatrix} g_{\lambda_1}(x_i) \\ -g_{\lambda_2}(x_i) \end{pmatrix}^t \begin{pmatrix} \Sigma_{\text{pred},-i}(\lambda_1, \lambda_1) & \Sigma_{\text{pred},-i}(\lambda_1, \lambda_2) \\ \Sigma_{\text{pred},-i}(\lambda_2, \lambda_1) & \Sigma_{\text{pred},-i}(\lambda_2, \lambda_2) \end{pmatrix} \begin{pmatrix} g_{\lambda_1}(x_i) \\ -g_{\lambda_2}(x_i) \end{pmatrix}. \quad (78)$$

We can compute an empirical coverage probability for 0 at level  $1 - \alpha$  using  $N$  i.i.d. sample pairs  $(\lambda_1, \lambda_2) \sim \pi(\lambda|w) \times \pi(\lambda|w)$ :

$$\hat{\Delta}(\alpha, x_i) = \frac{1}{N} \sum_{j=1}^N \mathbf{1}_{\{0 \in [\mu_i(\lambda_{1,j}, \lambda_{2,j}) \pm q_{1-\alpha/2} \sqrt{\sigma_i^2(\lambda_{1,j}, \lambda_{2,j})}]\}}, \quad (79)$$

where  $q_{1-\alpha/2}$  denotes the  $(1 - \alpha/2)$  quantile of the standard Gaussian distribution. One expects  $\hat{\Delta}(\alpha, x_i)$  to be close to  $1 - \alpha$ . When  $\alpha = 5\%$ , the presence of a compensation effect should be questioned whenever  $\hat{\Delta}(5\%, x_i)$  is significantly below 95%.

Investigating the presence of a compensation effect may justify the use of the cut approach rather than the full approach, even in situations where the latter is theoretically optimal, i.e., when the modeling assumptions of Eq. (4) are fully satisfied (no model discrepancy and Gaussian experimental uncertainty). In this well-specified framework, although the cut posterior differs from the full posterior, this discrepancy is expected to have only a limited impact on the predictive distribution of the chained model when a compensation effect is present.

## 5 Numerical examples

### 5.1 One-dimensional examples

To illustrate the performance of the GP-LinCC method, we start with the example in Eq. (11) introduced in Section 2.2. Recall that the posterior distribution  $\pi(\lambda|w)$  is

Gaussian,  $\mathcal{N}(\mu_{\lambda,\text{cut}}, \sigma_{\lambda,\text{cut}}^2)$ , with mean and variance given by

$$\mu_{\lambda,\text{cut}} = \bar{w}, \quad \sigma_{\lambda,\text{cut}}^2 = \frac{\sigma_w^2}{n_1}. \quad (80)$$

where  $n_1 = 15$  denotes the size of the vector  $w$ .

The functional parameter  $\theta(\lambda) \in \mathbb{R}$  is assumed to follow a GP with a constant mean function  $m_\beta(\lambda) = \beta$  and a Matérn 5/2 covariance function given by Eq. (29). The quantities  $g_{\lambda,0}(x_i)$  and  $g_{\lambda,1}(x_i)$  introduced in Section 4 are therefore  $x_i\lambda$  and 1, respectively. Note that, by construction of GP–LinCC, the predictive distribution  $\pi_{\text{pred}}(\theta(\lambda)|\bar{\mathbf{z}}, \phi)$  interpolates the posterior mean of  $\theta|\lambda$ , which is

$$\mu_{\theta|\lambda} := \bar{z} - \bar{x}\lambda. \quad (81)$$

Since Eq. (81) forms a perfectly linear function of  $\lambda$ , interpolating it with a smooth Matérn 5/2 GP leads to an almost collinear covariance matrix, causing numerical conditioning issues [35] and making the resulting GP–LinCC predictive distribution unreliable. To address this, we apply the bounded, smooth reparameterization  $T : \mathbb{R} \rightarrow ]-1, 1[$ , which moves the linear posterior means onto a non-linear scale on which the covariance matrix is well conditioned:

$$\begin{aligned} T(a) &= \frac{2}{1 + e^{-a}} - 1 = \frac{e^a - 1}{e^a + 1} = \tanh\left(\frac{a}{2}\right), & a \in \mathbb{R}, \\ T^{-1}(b) &= \log\left(\frac{1+b}{1-b}\right) = 2 \operatorname{arctanh}(b), & b \in ]-1, 1[. \end{aligned} \quad (82)$$

We can apply the GP–LinCC approach to the transformed parameter  $\eta(\lambda) := T(\theta(\lambda))$ . The design  $D_m$  is constructed by mapping an LHS  $m$ -sample on  $[0, 1]$  onto  $\pi(\lambda|w)$  via the inverse standard normal CDF. Let  $\tilde{\pi}_{\text{pred}}(\eta(\lambda)|\bar{\mathbf{z}}, \phi)$  denote the resulting predictive distribution of  $\eta(\lambda)$ . By a change of variables through  $T^{-1}$ , the induced predictive distribution of  $\theta(\lambda)$  is obtained by applying an  $\operatorname{arctanh}$  transformation to a Gaussian predictive law, which yields a non-standard distribution that can be referred to as *tanh-normal*:

$$\pi_{\text{pred}}(\theta(\lambda)|\bar{\mathbf{z}}, \phi) = \tilde{\pi}_{\text{pred}}\left(\frac{e^{\theta(\lambda)} - 1}{e^{\theta(\lambda)} + 1} \middle| \bar{\mathbf{z}}, \phi\right) \left(\frac{2e^{\theta(\lambda)}}{(e^{\theta(\lambda)} + 1)^2}\right). \quad (83)$$

The GP hyperparameters  $\phi = (\beta, \psi, \sigma^2)$  are estimated by marginal likelihood maximization (see Eq. (56)).

For each sampled pair  $(\lambda_{1,j}, \lambda_{2,j})$  in Eq. (79), the empirical coverage probability is computed as follows:

1. Draw  $N_\theta$  samples from the GP–LinCC predictive distribution associated with  $(\eta(\lambda_{1,j}), \eta(\lambda_{2,j}))$ .
2. Apply  $T^{-1}$  to these  $N_\theta$  samples to obtain draws of  $(\theta(\lambda_{1,j}), \theta(\lambda_{2,j}))$ .

3. For each draw, compute

$$Z_{ij} := x_i(\lambda_{1,j} - \lambda_{2,j}) + \theta(\lambda_{1,j}) - \theta(\lambda_{2,j}). \quad (84)$$

4. Compute the empirical quantiles  $q_{\alpha/2}^{ij}$  and  $q_{1-\alpha/2}^{ij}$  from the  $N_\theta$  values of  $Z_{ij}$ .

Finally,

$$\hat{\Delta}(\alpha, x_i) = \frac{1}{N} \sum_{j=1}^N \mathbf{1}_{\{0 \in [q_{\alpha/2}^{ij}, q_{1-\alpha/2}^{ij}]\}}. \quad (85)$$

For each fixed  $\lambda$ , the model output is equal to

$$r_i(\lambda) := x_i \lambda + \theta(\lambda). \quad (86)$$

Since the predictive distribution of  $\theta(\lambda)$  is *tanh-normal*, the distribution of  $r_i(\lambda) = x_i \lambda + \theta(\lambda)$  is the corresponding translated *tanh-normal* distribution, with density

$$\pi(r_i(\lambda) | \vec{\mathbf{z}}_{-i}, \phi) = \tilde{\pi}_{\text{pred}} \left( \frac{e^{r_i(\lambda) - x_i \lambda} - 1}{e^{r_i(\lambda) - x_i \lambda} + 1} \mid \vec{\mathbf{z}}_{-i}, \phi \right) \left( \frac{2 e^{r_i(\lambda) - x_i \lambda}}{(e^{r_i(\lambda) - x_i \lambda} + 1)^2} \right). \quad (87)$$

We consider the two settings introduced in Section 2.2:

- Non-identifiable setting:  $x_i = 5$  for  $1 \leq i \leq n = 15$ .
- Identifiable setting:  $x_i \sim \mathcal{U}(-6, 6)$  for  $1 \leq i \leq n = 15$ .

In each setting, GP-LinCC is applied as previously described, and the resulting predictive cut distribution is compared with the target cut distribution obtained under the Jeffreys prior  $\pi(\theta|\lambda) \propto 1$ .

### 5.1.1 Non-identifiable setting

We constructed a design  $D_m$  of size  $m = 10$ . Figure 5 displays a comparison between the KDE of the target conditional density  $\pi(\theta|z, \lambda)$  and the predictive tanh-normal density  $\pi_{\text{pred}}(\theta(\lambda)|\vec{\mathbf{z}}, \hat{\phi})$  for the value  $\lambda = 1.238$ . The predictive density is close to the target conditional density, especially in terms of location, although it underestimates its dispersion. Similar behavior is observed for other draws of  $\lambda \sim \pi(\lambda|w)$ . Figure 6 presents a comparison between the target cut distribution given in Eq. (7) and the predictive cut distribution obtained by replacing  $\pi(\theta|z, \lambda)$  with  $\pi_{\text{pred}}(\theta(\lambda)|\vec{\mathbf{z}}, \hat{\phi})$ . The two distributions show good agreement. However, the predictive cut distribution is less accurate in the tails of the support of  $\lambda$ . This occurs because  $\pi(\lambda|w)$  concentrates most of its mass around its mean, so the LHS-based design  $D_m$  contains fewer points in the tails.

In addition, Figure 7 shows the boxplots of the IMSE criterion for different sizes of  $D_m$  and for a fixed sample  $z$  of size  $n = 15$ . These boxplots, associated with each design, are obtained from 1000 samples of the conditional distribution  $\pi(\theta|z, \lambda)$  and the conditional distribution  $\pi_{\text{pred}}(\theta(\lambda)|\vec{\mathbf{z}}, \hat{\phi})$  provided by GP-LinCC approach. As the size

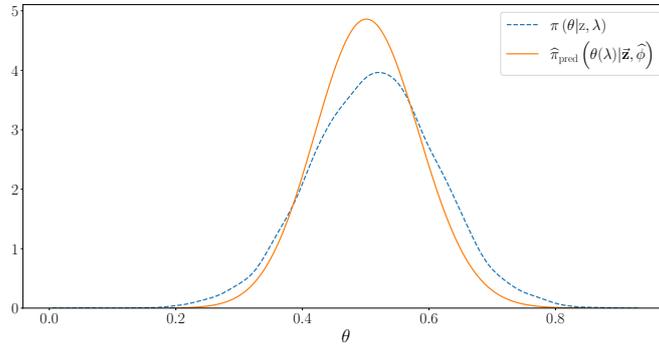


Figure 5: Case  $x_i = 5$  ( $1 \leq i \leq n = 15$ ). Comparison between the target conditional density  $\pi(\theta|z, \lambda)$  under the Jeffreys prior on  $\theta$  and the tanh-normal density  $\pi_{\text{pred}}(\theta(\lambda)|\bar{\mathbf{z}}, \hat{\phi})$  obtained using a design  $D_m$  with  $m = 10$ , for  $\lambda = 1.238$ .  $\hat{\pi}_{\text{pred}}(\cdot|\cdot)$  denotes the KDE of  $\pi_{\text{pred}}(\cdot|\cdot)$ .

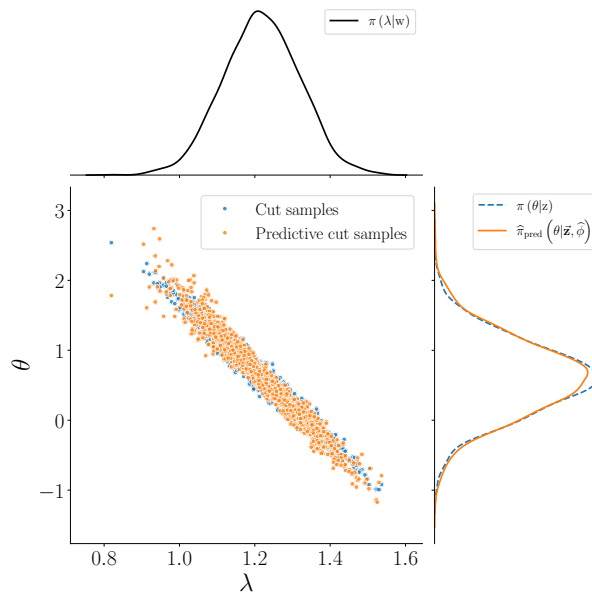


Figure 6: Case  $x_i = 5$  ( $1 \leq i \leq n = 15$ ). Comparison between the target cut distribution under the Jeffreys prior on  $(\lambda, \theta)$  and the GP-LinCC predictive cut distribution combined with  $T^{-1}$ , using a design  $D_m$  of size  $m = 10$ . For each distribution, 2000 samples are displayed.

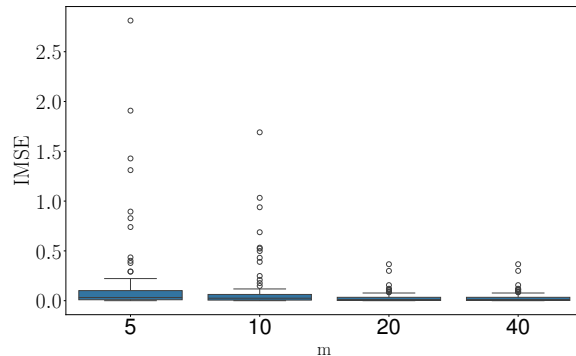


Figure 7: Case  $x_i = 5$  ( $1 \leq i \leq n = 15$ ). Boxplot of the IMSE criterion for different sizes  $m \in \{5, 10, 20, 40\}$  of  $D_m$  and for a fixed sample  $z$  of size  $n = 15$ . Each boxplot is obtained from 1000 samples.

$m$  of  $D_m$  increases, the IMSE decreases, highlighting the good predictive ability of the GP–LinCC approach.

A compensation effect was expected due to the non-identifiability of the model. To assess this, the empirical coverage probabilities in Eq. (85) were computed with  $\alpha = 5\%$ , using  $N = 5000$  sample pairs  $(\lambda_1, \lambda_2)$  generated from  $\pi(\lambda|w)$  and  $N_\theta = 5000$  samples of  $\theta$  drawn from the GP–LinCC predictive distribution at  $(\lambda_1, \lambda_2)$ . The results exceeded 95%, confirming the presence of a compensation effect.

### 5.1.2 Identifiable setting

In this identifiable configuration, Figures 8, 9 and 10 show that GP–LinCC still provides an accurate approximation of the target cut distribution. As expected, the compensation effect no longer arises when the model is identifiable. This is reflected in the empirical coverage probabilities  $\hat{\Delta}(\alpha, x_i)$  displayed in Figure 11(a), which remain below the 95% threshold for most values of  $x_i$ .

For values of  $x_i$  close to the sample mean  $\bar{x}$ , the coverage may nevertheless exceed 95%. This does not indicate a compensation effect. Indeed, when  $x_i \approx \bar{x}$ , the term  $x_i(\lambda_1 - \lambda_2)$  becomes numerically close to  $-\bar{x}(\lambda_1 - \lambda_2)$ , which is the difference between the posterior means  $\mu_{\theta|\lambda_1} - \mu_{\theta|\lambda_2}$ . Because the posterior dispersion of  $\theta(\lambda)$  is small, the stochastic difference  $\theta(\lambda_1) - \theta(\lambda_2)$  in Eq. (84) remains close to the difference between these posterior means. Consequently, the two contributions in  $Z_{ij}$  nearly cancel each other. As a result,  $Z_{ij}$  concentrates near zero for such  $x_i$ , yielding local coverage rates above 95% even though no compensation effect is present.

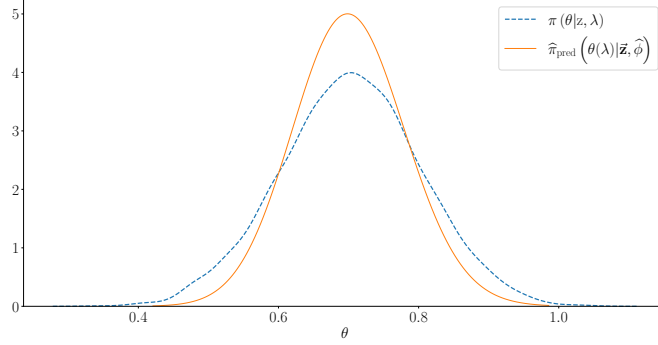


Figure 8: Case  $x_i \sim \mathcal{U}(-6, 6)$  ( $1 \leq i \leq n = 15$ ). Comparison between the target conditional density  $\pi(\theta|z, \lambda)$  under the Jeffreys prior on  $\theta$  and the tanh-normal density  $\pi_{\text{pred}}(\theta(\lambda)|\bar{\mathbf{z}}, \hat{\phi})$  obtained using a design  $D_m$  with  $m = 10$ , for  $\lambda = 1.227$ .

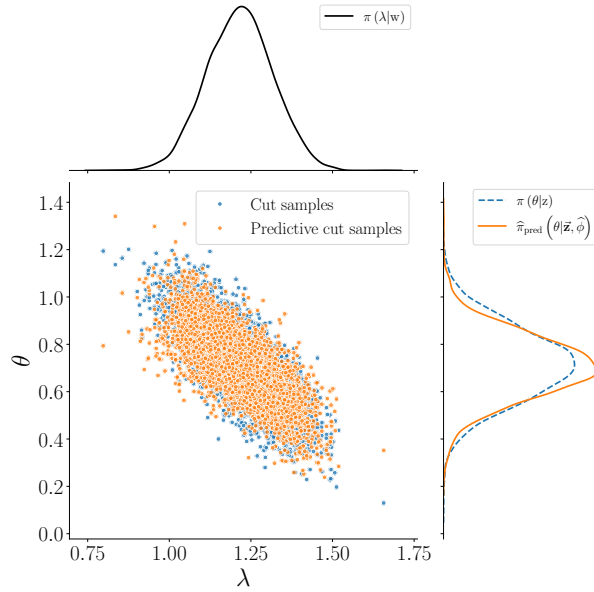


Figure 9: Case  $x_i \sim \mathcal{U}(-6, 6)$  ( $1 \leq i \leq n = 15$ ). Comparison between the target cut distribution under the Jeffreys prior on  $(\lambda, \theta)$  and the GP-LinCC predictive cut distribution combined with  $T^{-1}$ , using a design  $D_m$  of size  $m = 10$ . For each distribution, 2000 samples are displayed.

## 5.2 A two-dimensional example

We consider the following example:

$$\begin{cases} w_j = \lambda + \epsilon_{w_j} & ; \quad \epsilon_{w_j} \sim \mathcal{N}(0, \sigma_w^2), \\ z_i = g_{\lambda,0}(x_i) + g_{\lambda,1}(x_i)\theta + \epsilon_{z_i} & ; \quad \epsilon_{z_i} \sim \mathcal{N}(0, \sigma_z^2), \end{cases} \quad (88)$$

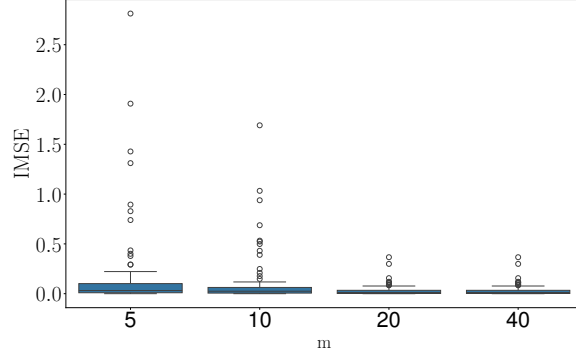


Figure 10: Case  $x_i \sim \mathcal{U}(-6, 6)$  ( $1 \leq i \leq n = 15$ ). Boxplot of the IMSE criterion for different sizes  $m \in \{5, 10, 20, 40\}$  of  $D_m$  and for a fixed sample  $z$  of size  $n = 15$ . Each boxplot is obtained from 1000 samples.

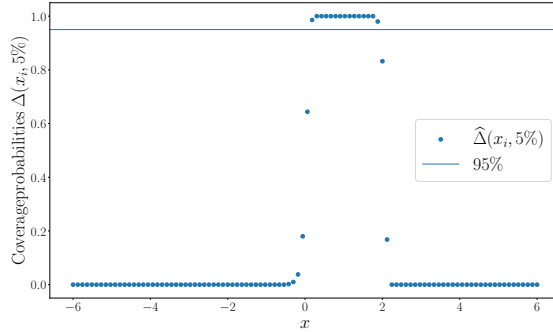


Figure 11: Empirical coverage probabilities  $\hat{\Delta}(\alpha, x_i)$  (Eq. (85), 100 sampled  $x_i$ ).

where

$$g_{\lambda,0}(x_i) = (\lambda + 1) \sin(20\lambda + 1), \quad g_{\lambda,1}(x_i) = (x_i + 1, x_i^2 - 1), \quad \theta = \begin{pmatrix} \theta_1 \\ \theta_2 \end{pmatrix}, \quad (89)$$

and  $\sigma_z^2 = 0.1$ ,  $\sigma_w^2 = 0.2$ , while  $x_i \sim \mathcal{U}[0, 3]$  for  $1 \leq i \leq n = 30$ . The marginal cut posterior density  $\pi(\lambda|w)$  is still Gaussian,

$$\pi(\lambda|w) \sim \mathcal{N}(\mu_{\lambda,\text{cut}}, \sigma_{\lambda,\text{cut}}^2), \quad \mu_{\lambda,\text{cut}} = \bar{w}, \quad \sigma_{\lambda,\text{cut}}^2 = \frac{\sigma_w^2}{n_1}, \quad (90)$$

where  $n_1 = 30$  is the size of  $w$ . GP-LinCC is implemented by assigning to each component of  $\theta(\lambda)$  a Matérn 5/2 Gaussian process with constant mean, consistent with the assumptions used throughout the paper.

Figure 12 compares, as a function of  $\lambda$ , the two marginal densities extracted from  $\pi(\theta|\lambda, z)$  with the corresponding predictive conditional densities obtained by GP-LinCC

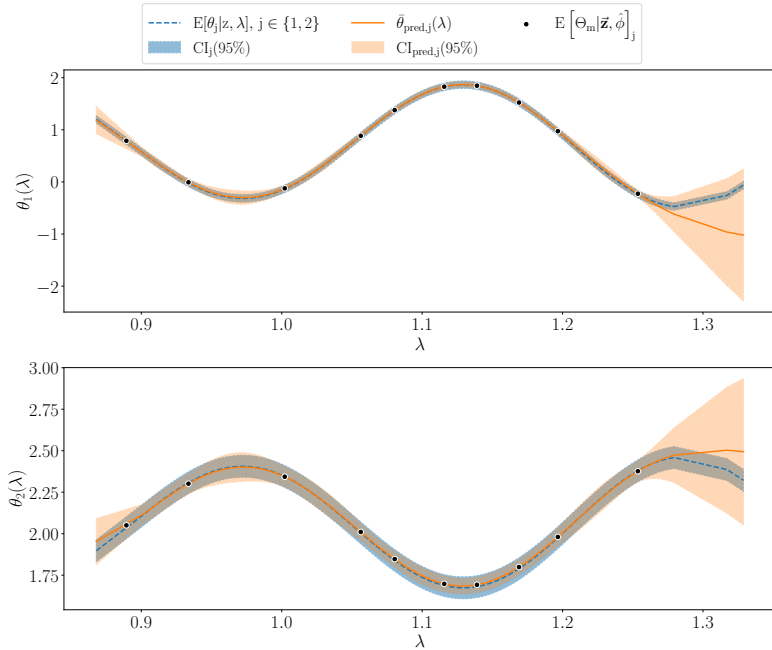


Figure 12: Comparison between the target conditional expectations  $\mathbb{E}[\theta_j|\lambda, z]$  computed under  $\pi(\theta|\lambda) \propto 1$  and their GP-LinCC predictive counterparts  $\bar{\theta}_{\text{pred},j}(\lambda)$ , shown with 95% credible intervals. The top panel displays  $\theta_1$  and the bottom panel  $\theta_2$  ( $n = 30$ ,  $m = 10$ ).

using  $n = 30$  observations. The predictive 95% predictive intervals for  $\theta_1(\lambda)$  and  $\theta_2(\lambda)$  cover their target posterior means  $\mathbb{E}[\theta_1|\lambda, z]$  and  $\mathbb{E}[\theta_2|\lambda, z]$  reasonably well, although the accuracy decreases near the boundaries of the  $\lambda$ -domain. In fact, outside the range covered by the training samples, the GP-LinCC predictor operates in extrapolation, resulting in increasing deviations and widening predictive intervals. Figure 13 then compares the target and predictive cut distributions, showing that the covariance structure of  $(\theta_1, \theta_2)$  as a function of  $\lambda$  is also well reproduced by GP-LinCC. Finally, Figure 14 reports the empirical coverage probabilities  $\hat{\Delta}(5\%, x_i)$ . As expected in this identifiable setting, the diagnostic confirms the absence of a compensation effect.

## 6 Conclusion

In this paper, we have presented a new method to tackle the computation of a cut distribution within the framework of Bayesian calibration of two chained numerical models. Favoring such a distribution makes sense in multiphysics simulation where some experimental data may be unable to inform adequately part of the uncertain parameters of the numerical chain. By assuming that the probability distribution of the parameter  $\lambda$  is known, the method, called GP-LinCC, amounts to estimating the parameters  $\theta$  of the downstream model conditionally on both the associated experimental data and the pa-

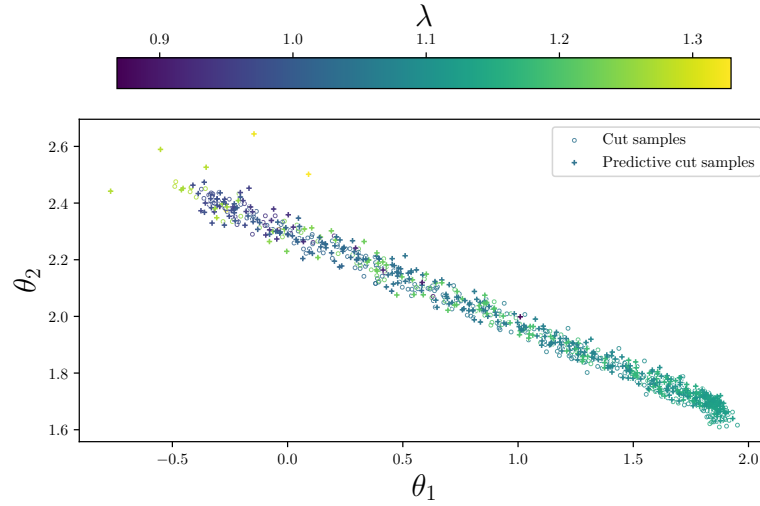


Figure 13: Comparison between the target cut distribution  $\pi_{\text{cut}}(\theta_1, \theta_2, \lambda|w, z)$  and the corresponding predictive distribution  $\pi_{\text{cut,pred}}(\theta_1, \theta_2, \lambda|w, \vec{z}, \phi)$  computed by GP-LinCC.

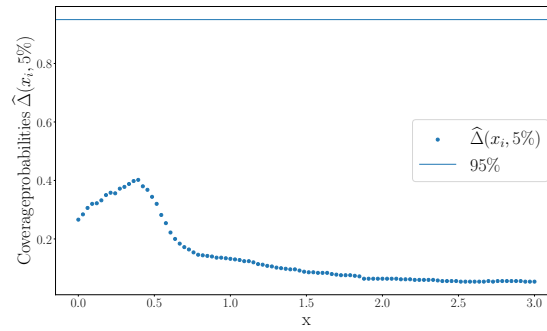


Figure 14: (2-D example) Empirical coverage probabilities  $\hat{\Delta}(\alpha, x_i)$  (Eq. (79), 100 sampled  $x_i$ ).

parameters  $\lambda$  of the upstream model. This conditional distribution is derived from Bayes' theorem in which a Gaussian process prior is specified for the calibration function  $\theta(\lambda)$  and the likelihood relies on a numerical design of the downstream model associated with a set  $D_m$  of realizations for  $\lambda$ . As a result, GP-LinCC offers an analytical Gaussian posterior distribution provided that the downstream model is assumed to be a linear function of  $\theta$ , thus avoiding the use of an MCMC algorithm. We further showed that GP-LinCC yields an analytically Gaussian predictive distribution for  $\theta(\lambda^*)$  for any new realization  $\lambda^* \notin D_m$ .

GP-LinCC has been applied to some academic examples in low dimension for the parameter  $\theta$ , and the results obtained are convincing. Across these examples, the numerical experiments confirm that GP-LinCC provides accurate approximations of the exact conditional distribution  $\pi(\theta|\lambda, z)$  involved in the cut formulation. The main discrepancies in fact occur near the extremes of the posterior support of  $\lambda$ , where the LHS design mapped through the Gaussian quantile function becomes quite sparse. These discrepancies can be mitigated by increasing the size of  $D_m$ , which overall reduces the gap between the exact and predictive cut distributions. However, the gap does not converge to 0 because the GP-LinCC predictive distribution is structurally different from the exact conditional  $\pi(\theta|\lambda, z)$ . The former relies on a Gaussian process approximation of  $\theta(\lambda)$ , combined with empirical-Bayes hyperparameter estimation.

Several avenues for future work can be identified. First, the parameters  $\theta$  may have bounded variation ranges related to their physical meaning. It would therefore be necessary to incorporate such bound constraints within the GP-LinCC framework to ensure that the method remains consistent when applied to real physical problems. In this case, the predictive distribution delivered by GP-LinCC becomes a truncated multivariate normal distribution [11, 28]. Another important aspect concerns the impact of linearization errors. In GP-LinCC, they are globally modelled through the scale parameters that capture the portion of variance unexplained by the linear emulators of the downstream model, but a more explicit assessment of their influence on the resulting cut distribution would be valuable. With highly time-consuming simulations, it would also be useful to develop adaptive designs for the set  $D_m$  to improve the efficiency of the method. Finally, extending GP-LinCC to accommodate non-linear downstream models would further enhance its applicability and robustness for complex real-world problems.

We plan to apply the GP-LinCC method to the fuel application for pressurized water reactors that has motivated this methodological work, namely the calibration of the parameters of the fission gas behavior model conditionally on the thermal conductivity. However, a preliminary sensitivity analysis must be performed before deploying GP-LinCC on this physical problem. Indeed, the large dimension of  $\theta$  (more than ten parameters) requires a pre-selection of the most influential parameters. To achieve this, we carried out a global sensitivity analysis using the multivariate version of the sensitivity indices based on the Hilbert–Schmidt independence criterion (HSIC) [3].

## Acknowledgments

This work was partly funded under a tripartite project on Uncertainty Quantification between the French Alternative Energies and Atomic Energy Commission (CEA), Électricité de France (EDF), and Framatome (FRA). We thank Merlin Keller, research engineer at EDF R&D, for insightful discussions on cut-off models, which contributed to the mathematical formalization of the calibration problem.

## Declaration of generative AI and AI-assisted technologies in the manuscript preparation process

During the preparation of this work, the authors used ChatGPT (OpenAI) in order to improve the English language and readability of the manuscript. After using this tool, the authors reviewed and edited the content as needed and take full responsibility for the content of the published article.

## References

- [1] M. Avramova, A. Abarca, J. Hou, and K. Ivanov. Innovations in multi-physics methods development, validation, and uncertainty quantification. *Journal of Nuclear Engineering*, 2(1):44–56, 2021.
- [2] F. Bachoc. *Parametric estimation of covariance function in Gaussian-process based Kriging models. Application to uncertainty quantification for computer experiments*. PhD thesis, Université Paris-Diderot, 2013.
- [3] O. Baldé, G. Sarazin, A. Marrel, G. Damblin, and A. Bouloré. Kernel-based parameter screening for conditional Bayesian calibration of chained numerical models: application to fuel performance simulation of pressurized water reactors. HAL preprint, Sept. 2025.
- [4] S. Barratt. A matrix Gaussian distribution. *arXiv preprint arXiv:1804.11010*, 2018.
- [5] N. Bousquet, M. Blazère, and T. Cerbelaud. Covariance constraints for stochastic inverse problems of computer models. *Electronic Journal of Statistics*, 19(1):1809–1854, 2025.
- [6] D. A. Brown and S. Atamturktur. Nonparametric functional calibration of computer models. *Statistica Sinica*, pages 721–742, 2018.
- [7] K. Campbell. Statistical calibration of computer simulations. *Reliability Engineering and System Safety*, 91(10–11):1358–1363, 2006.
- [8] X. Chen, O. Linton, and P. Robinson. The estimation of conditional densities. Econometrics Paper Series EM/01/415, STICERD, London School of Economics, 2001.

- [9] D. Cole. *Parameter Redundancy and Identifiability*. CRC Press, 2020.
- [10] C. Currin, T. J. Mitchell, M. Morris, and D. Ylvisaker. Bayesian prediction of deterministic functions, with applications to the design and analysis of computer experiments. *Journal of the American Statistical Association*, 86(416):953–963, 1991.
- [11] S. Da Veiga and A. Marrel. Gaussian process regression with linear inequality constraints. *Reliability Engineering & System Safety*, 195:106732, 2020.
- [12] G. Damblin and P. Gaillard. Bayesian inference and non-linear extensions of the circe method for quantifying the uncertainty of closure relationships integrated into thermal-hydraulic system codes. *Nuclear Engineering and Design*, 359:110391, 2020.
- [13] G. Damblin, P. Barbillon, M. Keller, A. Pasanisi, and É. Parent. Adaptive numerical designs for the calibration of computer codes. *SIAM/ASA Journal on Uncertainty Quantification*, 6(1):151–179, 2018.
- [14] E. DeCarlo, B. Smarslok, and S. Mahadevan. Segmented Bayesian calibration of multidisciplinary models. *AIAA Journal*, 54(12):3727–3741, 2016.
- [15] G. Delipei, J. Garnier, J.-C. Le Pallec, and B. Normand. Multi-physics uncertainties propagation in a PWR rod ejection accident modeling - analysis methodology and first results. In *BEPU Conference*, 2018.
- [16] P. Fiszeder and W. Orzeszko. Covariance matrix forecasting using support vector regression. *Applied Intelligence*, 51(10):7029–7042, 2021.
- [17] M. Gu, X. Wang, and J. O. Berger. Robust Gaussian stochastic process emulation. *The Annals of Statistics*, 46(6A):3038–3066, 2018.
- [18] G. Han, T. J. Santner, and J. J. Rawlinson. Simultaneous determination of tuning and calibration parameters for computer experiments. *Technometrics*, 51(4):464–474, 2009.
- [19] C. Introïni, I. Ramière, J. Sercombe, B. Michel, T. Helfer, and J. Fauque. ALCY-ONE: the fuel performance code of the PLEIADES platform dedicated to PWR fuel rods behavior. *Annals of Nuclear Energy*, 207:110711, 2024.
- [20] P. Jacob, J. O’Leary, and Y. Atchadé. Unbiased markov chain monte carlo with couplings (with discussion). *Journal of the Royal Statistical Society: Series B*, 82: 543–600, 2020.
- [21] P. E. Jacob, L. M. Murray, C. C. Holmes, and C. P. Robert. Better together? statistical learning in models made of modules. *arXiv preprint arXiv:1708.08719*, 2017.
- [22] M. C. Kennedy and A. O’Hagan. Bayesian calibration of computer models. *Journal of the Royal Statistical Society: Series B*, 63(3):425–464, 2001.

- [23] K. Kzyurova, J. Berger, and R. Wolpert. Coupling computer models through linking their statistical emulators. *SIAM/ASA Journal on Uncertainty Quantification*, 6(3):1151–1171, 2018.
- [24] Q. Li and J. S. Racine. *Nonparametric Econometrics: Theory and Practice*. Princeton University Press, 2007.
- [25] F. Liu, M. Bayarri, and J. Berger. Modularization in Bayesian analysis, with emphasis on analysis of computer models. *Bayesian Analysis*, 4(1):119–150, 2009.
- [26] Y. Liu and R. J. Goudie. Stochastic approximation cut algorithm for inference in modularized Bayesian models. *Statistics and Computing*, 32(1):7, 2022.
- [27] J. Loepky, D. Bingham, and W. Welch. Computer model calibration or tuning in practice. Technical report, University of British Columbia, 2006.
- [28] A. F. López-Lopera, F. Bachoc, N. Durrande, and O. Roustant. Finite-dimensional Gaussian approximation with linear inequality constraints. *SIAM/ASA Journal on Uncertainty Quantification*, 6(3):1224–1255, 2018.
- [29] S. Marque-Pucheu, G. Perrin, and J. Garnier. Calibration of nested computer models. In *VII European Congress on Computational Methods in Applied Sciences and Engineering (ECCOMAS Congress), Crete Island*, 2016.
- [30] S. Marque-Pucheu, G. Perrin, and J. Garnier. Calibration and prediction of two nested computer codes. HAL preprint, Jul 2017.
- [31] A. Marrel, B. Iooss, and V. Chabridon. The ICSCREAM methodology: identification of penalizing configurations in computer experiments using screening and metamodel—applications in thermal hydraulics. *Nuclear Science and Engineering*, 196(3):301–321, 2022.
- [32] M. McKay, R. Beckman, and W. Conover. A comparison of three methods for selecting values of input variables in the analysis of output from a computer code. *Technometrics*, 21(2):239–245, 1979.
- [33] D. Ming and S. Guillas. Linked Gaussian process emulation for systems of computer models using matern kernels and adaptive design. *SIAM/ASA Journal on Uncertainty Quantification*, 9(4):1615–1642, 2021.
- [34] H. Otneim. Multivariate and conditional density estimation using local Gaussian approximations. Technical report, University of Bergen, 2016.
- [35] C.-Y. Peng and C. F. J. Wu. On the choice of nugget in kriging modeling for deterministic computer experiments. *Journal of Computational and Graphical Statistics*, 23(1):151–168, 2014.
- [36] M. Plummer. Cuts in Bayesian graphical models. *Statistics and Computing*, 25: 37–43, 2015.

- [37] C. P. Robert and G. Casella. *Monte Carlo Statistical Methods*. Springer, 1999.
- [38] J. Sacks, W. J. Welch, T. J. Mitchell, and H. P. Wynn. Design and analysis of computer experiments. *Statistical Science*, 4(4):409–423, 1989.
- [39] F. Sanson, O. Le Maitre, and P. Congedo. Systems of gaussian process models for directed chains of solvers. *Computer Methods in Applied Mechanics and Engineering*, 352:32–55, 2019.
- [40] T. J. Santner, B. J. Williams, and W. I. Notz. *The design and analysis of computer experiments*. Springer, 2018.
- [41] C.-L. Sung and R. Tuo. A review on computer model calibration. *WIREs Computational Statistics*, 16(1):e1645, 2024.
- [42] C. K. Williams and C. E. Rasmussen. *Gaussian processes for machine learning*, volume 2. MIT press Cambridge, MA, 2006.
- [43] X. Wu, T. Kozłowski, H. Meidani, and K. Shirvan. Inverse uncertainty quantification using the modular Bayesian approach based on Gaussian process, Part 1: Theory. *Nuclear Engineering and Design*, 335:339–355, 2018.
- [44] J. Ye, M. Mahmoudi, K. Karayagiz, L. Johnson, R. Seede, I. Karaman, R. Arroyave, and A. Elwany. Bayesian calibration of multiple coupled simulation models for metal additive manufacturing: A Bayesian network approach. *ASCE-ASME Journal of Risk and Uncertainty in Engineering Systems, Part B: Mechanical Engineering*, 8(1):011111, 2022.
- [45] K. Zeng, J. Hou, K. Ivanov, and M. Jessee. Uncertainty quantification and propagation of multiphysics simulation of the pressurized water reactor core. *Nuclear Technology*, 205(12):1618–1637, 2019.

## Appendix A. Some useful mathematical results

### A.1 Vectorization

Vectorization transforms any matrix  $A \in \mathbb{R}^{m \times p}$  into a column vector  $\vec{A} \in \mathbb{R}^{mp}$  obtained by stacking the columns of  $A$ . For example,

$$A = \begin{pmatrix} a & b \\ c & d \end{pmatrix} \quad \Rightarrow \quad \vec{A} = \begin{pmatrix} a \\ c \\ b \\ d \end{pmatrix}. \quad (\text{A.1.1})$$

### A.2 Gaussian process

A Gaussian process (GP) is a collection of random variables such that any finite subset follows a multivariate normal distribution. Suppose that we observe

$$\Theta_m = (\theta(\lambda_j))_{1 \leq j \leq m}^t \in \mathbb{R}^m. \quad (\text{A.2.1})$$

with  $\theta(\lambda_j) \in \mathbb{R}$ ,  $\lambda_j \in \mathbb{R}^q$  for some  $q \geq 1$ , and a design

$$D_m = (\lambda_1, \dots, \lambda_m)^t. \quad (\text{A.2.2})$$

A GP prior is defined by its mean function  $m_\beta(\lambda)$  and its covariance function

$$C(\lambda, \lambda') := \sigma^2 K_\psi(\lambda, \lambda'),$$

where  $K_\psi(\cdot, \cdot)$  is a correlation function depending on hyperparameters  $\psi$ , and  $\sigma^2 > 0$  is a variance parameter.

Let  $\lambda^* \in \mathbb{R}^q$  denote a new input location. The joint distribution of  $\theta(\lambda^*)$  and  $\Theta_m$  is

$$\begin{pmatrix} \theta(\lambda^*) \\ \Theta_m \end{pmatrix} \sim \mathcal{N}_{m+1} \left( \begin{pmatrix} m_\beta(\lambda^*) \\ m_\beta(D_m) \end{pmatrix}, \begin{pmatrix} C(\lambda^*, \lambda^*) & C(\lambda^*, D_m) \\ C(\lambda^*, D_m)^t & C(D_m, D_m) \end{pmatrix} \right), \quad (\text{A.2.3})$$

where

$$m_\beta(D_m) = (m_\beta(\lambda_1), \dots, m_\beta(\lambda_m))^t, \quad (\text{A.2.4})$$

$$C(D_m, D_m) = (C(\lambda_i, \lambda_j))_{1 \leq i, j \leq m}, \quad (\text{A.2.5})$$

$$C(\lambda^*, D_m) = (C(\lambda^*, \lambda_j))_{1 \leq j \leq m}, \quad (\text{A.2.6})$$

$$C(D_m, \lambda^*) = C(\lambda^*, D_m)^t. \quad (\text{A.2.7})$$

By the standard conditioning formulas for multivariate normal distributions, assuming  $C(D_m, D_m)$  is nonsingular, the GP predictive mean at  $\lambda^*$  is

$$\bar{\theta}(\lambda^*) = m_\beta(\lambda^*) + C(\lambda^*, D_m) C(D_m, D_m)^{-1} (\Theta_m - m_\beta(D_m)), \quad (\text{A.2.8})$$

and the predictive covariance function is

$$\Sigma_{\text{pred}}(\lambda^*, \lambda^{*'}) = C(\lambda^*, \lambda^{*'}) - C(\lambda^*, D_m) C(D_m, D_m)^{-1} C(D_m, \lambda^{*'}). \quad (\text{A.2.9})$$

The above predictive covariance corresponds to the standard Gaussian process interpolation formulas assuming that the mean parameters  $\beta$  are fixed. If  $\beta$  were estimated jointly with the covariance hyperparameters, the predictive covariance would contain an additional correction term, as in universal kriging (see, e.g., [42]).

The hyperparameters  $\phi := (\beta, \sigma^2, \psi)$ , including regression and covariance parameters, are unknown in practice and are typically estimated by marginal likelihood maximization [42].

In this appendix section,  $\Theta_m$  is treated as observed to introduce the standard Gaussian process interpolation formulas. In contrast, it is a latent quantity in the GP–LinCC framework.

## Appendix B. Analytical example of Section 2

### B.1 Expression of cut and full distributions

We recall the statistical model,

$$\begin{pmatrix} w \\ z \end{pmatrix} = A_x \begin{pmatrix} \lambda \\ \theta \end{pmatrix} + \begin{pmatrix} \epsilon_w \\ \epsilon_z \end{pmatrix}. \quad (\text{B.1.1})$$

with

$$A_x = \begin{pmatrix} \mathbf{1}_{n_1} & \mathbf{0}_{n_1} \\ x & \mathbf{1}_{n_2} \end{pmatrix}, \quad x = (x_1, \dots, x_{n_2})^t. \quad (\text{B.1.2})$$

and

$$\begin{pmatrix} \epsilon_w \\ \epsilon_z \end{pmatrix} \sim \mathcal{N}_{n_1+n_2} \left( 0, \Sigma_\sigma := \begin{pmatrix} \sigma_w^2 I_{n_1} & 0 \\ 0 & \sigma_z^2 I_{n_2} \end{pmatrix} \right). \quad (\text{B.1.3})$$

#### Expression of the cut distribution $\pi_{\text{cut}}(\lambda, \theta|w, z)$

By Bayes formula, we have:

$$\pi(\theta|\lambda, z) \propto \mathcal{L}(z|\theta, \lambda) \pi(\theta), \quad (\text{B.1.4})$$

where

$$\mathcal{L}(z|\theta, \lambda) \propto \prod_{i=1}^{n_2} \exp\left(-\frac{1}{2\sigma_z^2} (z_i - (x_i \lambda + \theta))^2\right). \quad (\text{B.1.5})$$

After expansion of Eq. (B.1.4), we obtain:

1. For Gaussian prior on  $\theta$ :

$$\pi(\theta|\lambda, z) \sim \mathcal{N}(\mu_{\theta|\lambda, \text{cut}}, \sigma_{\theta, \text{cut}}^2). \quad (\text{B.1.6})$$

with

$$\sigma_{\theta, \text{cut}}^2 = \frac{\sigma_{\theta_0}^2 (\sigma_z^2/n_2)}{\sigma_{\theta_0}^2 + (\sigma_z^2/n_2)}, \quad \mu_{\theta|\lambda, \text{cut}} = \frac{\sigma_{\theta_0}^2 (\bar{z} - \bar{x}\lambda) + (\sigma_z^2/n_2)\theta_0}{\sigma_{\theta_0}^2 + (\sigma_z^2/n_2)}. \quad (\text{B.1.7})$$

2. For Jeffreys prior on  $\theta$ :

$$\pi(\theta|\lambda, z) \sim \mathcal{N}(\mu_{\theta|\lambda, \text{cut}}, \sigma_{\theta, \text{cut}}^2). \quad (\text{B.1.8})$$

with

$$\sigma_{\theta, \text{cut}}^2 = \frac{\sigma_z^2}{n_2}, \quad \mu_{\theta|\lambda, \text{cut}} = \bar{z} - \bar{x}\lambda. \quad (\text{B.1.9})$$

Note that, for Model 1 (i.e.,  $\forall 1 \leq i \leq n_2, x_i = c$ ), one has  $\bar{x} = c$ .  
Doing the same for  $\pi(\lambda|w)$ , one has:

1. For Gaussian prior on  $\lambda$ :

$$\pi(\lambda|w) \sim \mathcal{N}(\mu_{\lambda, \text{cut}}, \sigma_{\lambda, \text{cut}}^2). \quad (\text{B.1.10})$$

with

$$\mu_{\lambda, \text{cut}} = \frac{\sigma_{\lambda_0}^2 \bar{w} + (\sigma_w^2/n_1)\lambda_0}{\sigma_{\lambda_0}^2 + (\sigma_w^2/n_1)}, \quad \sigma_{\lambda, \text{cut}}^2 = \frac{\sigma_{\lambda_0}^2 (\sigma_w^2/n_1)}{\sigma_{\lambda_0}^2 + (\sigma_w^2/n_1)}. \quad (\text{B.1.11})$$

2. For Jeffreys prior on  $\lambda$ :

$$\pi(\lambda|w) \sim \mathcal{N}(\mu_{\lambda, \text{cut}}, \sigma_{\lambda, \text{cut}}^2). \quad (\text{B.1.12})$$

with

$$\mu_{\lambda, \text{cut}} = \bar{w}, \quad \sigma_{\lambda, \text{cut}}^2 = \frac{\sigma_w^2}{n_1}. \quad (\text{B.1.13})$$

Finally, the expression of  $\pi_{\text{cut}}(\theta, \lambda|w, z)$  is given by

$$\pi_{\text{cut}}(\theta, \lambda|w, z) \sim \mathcal{N}(\mu_{\theta|\lambda, \text{cut}}, \sigma_{\theta, \text{cut}}^2) \otimes \mathcal{N}(\mu_{\lambda, \text{cut}}, \sigma_{\lambda, \text{cut}}^2). \quad (\text{B.1.14})$$

**Expression of the full distribution**  $\pi_{\text{full}}(\lambda, \theta|w, z)$

From Bayes' rule:

$$\pi_{\text{full}}(\xi|w, z) \propto \mathcal{L}(w, z|\xi) \pi(\xi), \quad \xi = (\lambda, \theta)^t. \quad (\text{B.1.15})$$

1. **Gaussian prior on  $\xi$ .** The prior density is Gaussian:

$$\pi(\xi) \sim \mathcal{N}(\xi_0, \Sigma_0). \quad (\text{B.1.16})$$

Then

$$\pi_{\text{full}}(\xi|w, z) \sim \mathcal{N}(\Sigma v, \Sigma) \quad (\text{B.1.17})$$

with

$$v = A_x^t \Sigma_\sigma^{-1} \begin{pmatrix} w \\ z \end{pmatrix} + \Sigma_0^{-1} \xi_0, \quad \Sigma = (A_x^t \Sigma_\sigma^{-1} A_x + \Sigma_0^{-1})^{-1}. \quad (\text{B.1.18})$$

2. **Jeffreys prior on  $\xi$ .** The prior density is constant:

$$\pi(\xi) \propto 1. \quad (\text{B.1.19})$$

Then

$$\pi_{\text{full}}(\xi|w, z) \sim \mathcal{N}(\Sigma v, \Sigma) \quad (\text{B.1.20})$$

with

$$v = A_x^t \Sigma_\sigma^{-1} \begin{pmatrix} w \\ z \end{pmatrix}, \quad \Sigma = (A_x^t \Sigma_\sigma^{-1} A_x)^{-1}. \quad (\text{B.1.21})$$

We can then derive the marginal posterior of  $\lambda$ , which is also Gaussian:

$$\pi(\lambda|w, z) = \int \pi_{\text{full}}(\lambda, \theta|w, z) d\theta \sim \mathcal{N}((\Sigma v)_1, \Sigma_{11}). \quad (\text{B.1.22})$$

where  $(\Sigma v)_1$  stands for the first coordinate of the vector  $\Sigma v$ , that is the posterior mean of  $\lambda$ , and  $\Sigma_{11}$  denotes the first diagonal element of  $\Sigma$ , which is the posterior variance of  $\lambda$ .

## B.2 KL divergence between $\pi_{\text{cut}}(\lambda, \theta|w, z)$ and $\pi_{\text{full}}(\lambda, \theta|w, z)$

From Eq. (10), the KL divergence between  $\pi_{\text{cut}}(\lambda, \theta|w, z)$  and  $\pi_{\text{full}}(\lambda, \theta|w, z)$  reduces to the KL divergence between  $\pi(\lambda|w, z)$  and  $\pi(\lambda|w)$ , which are Gaussian distributions. The KL divergence is therefore

$$\text{KL}(\pi(\lambda|w, z) \parallel \pi(\lambda|w)) = \frac{1}{2} \log \left( \frac{\sigma_{\lambda, \text{cut}}^2}{\Sigma_{11}} \right) + \frac{1}{2} \frac{\Sigma_{11} + (\mu_{\lambda, \text{cut}} - (\Sigma v)_1)^2}{\sigma_{\lambda, \text{cut}}^2} - \frac{1}{2}. \quad (\text{B.2.1})$$

For Gaussian distributions, we know the following equivalence:

$$\text{KL}(\pi(\lambda|w, z) \parallel \pi(\lambda|w)) = 0 \iff (\Sigma v)_1 = \mu_{\lambda, \text{cut}} \quad \text{and} \quad \Sigma_{11} = \sigma_{\lambda, \text{cut}}^2. \quad (\text{B.2.2})$$

Let us see in which case Eq. (B.2.2) is satisfied. Based on the following expansion

$$\begin{aligned} A_x^t \Sigma_\sigma^{-1} A_x + \Sigma_0^{-1} &= \begin{pmatrix} \mathbf{1}_{n_1}^t & x^t \\ \mathbf{0}_{n_1}^t & \mathbf{1}_{n_2}^t \end{pmatrix} \begin{pmatrix} \sigma_w^{-2} I_{n_1} & \mathbf{0}_{n_1, n_2} \\ \mathbf{0}_{n_2, n_1} & \sigma_z^{-2} I_{n_2} \end{pmatrix} \begin{pmatrix} \mathbf{1}_{n_1} & \mathbf{0}_{n_1} \\ x & \mathbf{1}_{n_2} \end{pmatrix} + \Sigma_0^{-1} \\ &= \begin{pmatrix} n_1 \sigma_w^{-2} + \sigma_z^{-2} x^t x + \sigma_{\lambda_0}^{-2} & \sigma_z^{-2} x^t \mathbf{1}_{n_2} \\ \sigma_z^{-2} \mathbf{1}_{n_2}^t x & \sigma_z^{-2} n_2 + \sigma_{\theta_0}^{-2} \end{pmatrix} \end{aligned} \quad (\text{B.2.3})$$

the matrix  $\Sigma$  and the vector  $v$  are equal respectively to

$$\Sigma = \frac{1}{\det(A_x^t \Sigma_\sigma^{-1} A_x + \Sigma_0^{-1})} \begin{pmatrix} \sigma_z^{-2} n_2 + \sigma_{\theta_0}^{-2} & -\sigma_z^{-2} n_2 \bar{x} \\ -\sigma_z^{-2} n_2 \bar{x} & n_1 \sigma_w^{-2} + \sigma_z^{-2} n_2 \bar{x}^2 + \sigma_{\lambda_0}^{-2} \end{pmatrix} \quad (\text{B.2.4})$$

and

$$v = \begin{pmatrix} \sigma_w^{-2} n_1 \bar{w} + \sigma_z^{-2} x^t z + \sigma_{\lambda_0}^{-2} \lambda_0 \\ \sigma_z^{-2} n_2 \bar{z} + \sigma_{\theta_0}^{-2} \theta_0 \end{pmatrix}. \quad (\text{B.2.5})$$

Then, one has:

$$(\Sigma v)_1 = \frac{(\sigma_z^{-2} n_2 + \sigma_{\theta_0}^{-2}) (\sigma_w^{-2} n_1 \bar{w} + \sigma_z^{-2} x^t z + \sigma_{\lambda_0}^{-2} \lambda_0) - \sigma_z^{-2} n_2 \bar{x} (\sigma_z^{-2} \mathbf{1}_{n_2}^t z + \sigma_{\theta_0}^{-2} \theta_0)}{\det(A_x^t \Sigma_\sigma^{-1} A_x + \Sigma_0^{-1})} \quad (\text{B.2.6})$$

and

$$\Sigma_{11} = \frac{1}{\det(A_x^t \Sigma_\sigma^{-1} A_x + \Sigma_0^{-1})} (\sigma_z^{-2} n_2 + \sigma_{\theta_0}^{-2}). \quad (\text{B.2.7})$$

with

$$\det(A_x^t \Sigma_\sigma^{-1} A_x + \Sigma_0^{-1}) = \left[ (\sigma_z^{-2} n_2 + \sigma_{\theta_0}^{-2}) \times (n_1 \sigma_w^{-2} + \sigma_z^{-2} n_2 \bar{x}^2 + \sigma_{\lambda_0}^{-2}) \right] - (\sigma_z^{-2} n_2 \bar{x})^2. \quad (\text{B.2.8})$$

It follows that

$$\begin{aligned} \Sigma_{11} = \sigma_{\lambda, \text{cut}}^2 &\iff \\ &\frac{\sigma_z^{-2} n_2 + \sigma_{\theta_0}^{-2}}{(\sigma_z^{-2} n_2 + \sigma_{\theta_0}^{-2}) (n_1 \sigma_w^{-2} + \sigma_z^{-2} n_2 \bar{x}^2 + \sigma_{\lambda_0}^{-2}) - (\sigma_z^{-2} n_2 \bar{x})^2} \\ &= \frac{\sigma_{\lambda_0}^2 (\sigma_w^2 / n_1)}{\sigma_{\lambda_0}^2 + (\sigma_w^2 / n_1)} \\ &\iff (\sigma_z^{-2} n_2 + \sigma_{\theta_0}^{-2}) \sigma_z^{-2} n_2 \bar{x}^2 = (\sigma_z^{-2} n_2 \bar{x})^2 \\ &\iff (\sigma_z^{-2} n_2 + \sigma_{\theta_0}^{-2}) \bar{x}^2 = \sigma_z^{-2} n_2 \bar{x}^2. \end{aligned} \quad (\text{B.2.9})$$

Note that:

$$\frac{\sigma_z^{-2} n_2 + \sigma_{\theta_0}^{-2}}{\bar{x}^2} > \frac{\sigma_z^{-2} n_2}{\bar{x}^2}, \quad (\text{B.2.10})$$

(Jensen inequality in the discrete case).

Combining Eq. (B.2.9) with the above inequalities implies that

$$\bar{x}^2 = 0 \quad \text{and} \quad \bar{x}^2 = 0. \quad (\text{B.2.11})$$

Since  $\bar{x}^2 = \frac{1}{n_2} \sum_{i=1}^{n_2} x_i^2$ , this implies that  $x_i = 0$  for all  $1 \leq i \leq n_2$ . Therefore,

$$\left(\sigma_z^{-2} n_2 + \sigma_{\theta_0}^{-2}\right) \bar{x}^2 = \sigma_z^{-2} n_2 \bar{x}^2 \iff \forall 1 \leq i \leq n_2, x_i = 0. \quad (\text{B.2.12})$$

A similar computation shows that the condition  $(\Sigma v)_1 = \mu_{\lambda, \text{cut}}$  does not, by itself, impose  $x_i = 0$  for all  $i$ . However, once  $x_i = 0$  is enforced by the variance condition, one verifies that  $(\Sigma v)_1 = \mu_{\lambda, \text{cut}}$  automatically holds. Hence both conditions in Eq. (B.2.2) are simultaneously satisfied if and only if  $x_i = 0$  for all  $1 \leq i \leq n_2$ . Therefore, under a Gaussian prior, we have established the following result:

$$\text{KL}(\pi(\lambda|w, z) \parallel \pi(\lambda|w)) = 0 \iff \forall 1 \leq i \leq n_2, x_i = 0. \quad (\text{B.2.13})$$

For Jeffreys prior, following exactly the same reasoning as in the Gaussian-prior case, we obtain

$$\begin{aligned} \Sigma_{11} = \sigma_{\lambda, \text{cut}}^2 &\iff (\sigma_z^{-2} n_2) \bar{x}^2 = \sigma_z^{-2} n_2 \bar{x}^2 \\ &\iff \bar{x}^2 = \bar{x}^2 \\ &\iff \forall 1 \leq i \leq n_2, x_i = c \in \mathbb{R}. \end{aligned} \quad (\text{B.2.14})$$

As in the Gaussian prior case, the condition  $(\Sigma v)_1 = \mu_{\lambda, \text{cut}}$  does not, by itself, force  $x_i = c$  for all  $i$ . However, once  $x_i = c$  is imposed by the variance condition, one checks that  $(\Sigma v)_1 = \mu_{\lambda, \text{cut}}$  automatically holds. Therefore, both conditions in Eq. (B.2.2) are satisfied if and only if  $x_i = c$  for all  $1 \leq i \leq n_2$ . Thus, we have

$$\text{KL}(\pi(\lambda|w, z) \parallel \pi(\lambda|w)) = 0 \iff \forall 1 \leq i \leq n_2, x_i = c \in \mathbb{R}. \quad (\text{B.2.15})$$

## Appendix C. Proof of the results of Section 4

### C.1 Proof of Theorem 1

*Proof.* In the GP-LinCC framework, the vectorized parameter  $\vec{\Theta}_m$  stacks the  $p$  model parameters evaluated at the  $m$  design points, so that  $\vec{\Theta}_m \in \mathbb{R}^{pm}$ . Consequently, the covariance matrix  $\mathbf{C}_\phi$  is of dimension  $pm \times pm$ .

We consider the vectorized model

$$\vec{\mathbf{z}} = G \vec{\Theta}_m + \vec{\epsilon}, \quad \vec{\epsilon} \sim \mathcal{N}(0, \Sigma_{\vec{\epsilon}}), \quad (\text{C.1.1})$$

together with the Gaussian prior

$$\vec{\Theta}_m \sim \mathcal{N}(\vec{M}_\beta, \mathbf{C}_\phi). \quad (\text{C.1.2})$$

We assume that  $\mathbf{C}_\phi$  is symmetric positive definite, so that  $\mathbf{C}_\phi^{-1}$  exists. Since  $\vec{\epsilon}$  is independent of  $\vec{\Theta}_m$ , the joint vector

$$\begin{pmatrix} \vec{\Theta}_m \\ \vec{\mathbf{z}} \end{pmatrix} \quad (\text{C.1.3})$$

is multivariate normal with mean

$$\begin{pmatrix} \vec{M}_\beta \\ G\vec{M}_\beta \end{pmatrix} \quad (\text{C.1.4})$$

and block covariance matrix

$$\begin{pmatrix} \mathbf{C}_\phi & \mathbf{C}_\phi G^t \\ G\mathbf{C}_\phi & \Sigma_{\vec{e}} + G\mathbf{C}_\phi G^t \end{pmatrix}. \quad (\text{C.1.5})$$

The posterior distribution is therefore Gaussian, and its mean and covariance are obtained from the standard conditioning formulas for multivariate normal vectors:

$$\begin{aligned} \Sigma_\phi &= \left( \Delta^{-1} + \mathbf{C}_\phi^{-1} \right)^{-1}, \\ \mu_\phi &= \Sigma_\phi \left( G^t \Sigma_{\vec{e}}^{-1} \vec{z} + \mathbf{C}_\phi^{-1} \vec{M}_\beta \right). \end{aligned} \quad (\text{C.1.6})$$

with  $\Delta^{-1} := G^t \Sigma_{\vec{e}}^{-1} G$ . □

## C.2 Proof of Theorem 2

*Proof.* The predictive distribution of  $\theta(\lambda^*)$ , for a fixed  $\lambda^*$ , is defined by

$$\pi_{\text{pred}}(\vec{\theta}(\lambda^*) | \vec{z}, \phi) = \int_{\mathcal{T}^m} \pi(\vec{\theta}(\lambda^*) | \vec{\Theta}_m, \phi) \pi(\vec{\Theta}_m | \vec{z}, \phi) d\vec{\Theta}_m. \quad (\text{C.2.1})$$

Set  $\vec{\theta}^* := \vec{\theta}(\lambda^*)$ . From the GP prior specification, the joint vector

$$\begin{pmatrix} \vec{\Theta}_m \\ \vec{\theta}^* \end{pmatrix} \quad (\text{C.2.2})$$

is multivariate normal with mean

$$\begin{pmatrix} \vec{M}_\beta \\ \vec{m}_\beta(\lambda^*) \end{pmatrix} \quad (\text{C.2.3})$$

and block covariance matrix

$$\begin{pmatrix} \mathbf{C}_\phi & \mathbf{C}(D_m, \lambda^*) \\ \mathbf{C}(\lambda^*, D_m) & \mathbf{C}(\lambda^*, \lambda^*) \end{pmatrix}. \quad (\text{C.2.4})$$

By the standard conditioning formulas for multivariate normal distributions (see, e.g., Appendix A.2 in [42]), the conditional distribution of  $\theta^*$  given  $\vec{\Theta}_m$  and  $\phi$  is

$$\vec{\theta}^* | \vec{\Theta}_m, \phi \sim \mathcal{N}\left(\vec{m}_\beta(\lambda^*) + \mathbf{C}(\lambda^*, D_m) \mathbf{C}_\phi^{-1} (\vec{\Theta}_m - \vec{M}_\beta), \Sigma_{\text{cond}}(\lambda^*, \lambda^*)\right), \quad (\text{C.2.5})$$

with

$$\Sigma_{\text{cond}}(\lambda^*, \lambda^*) = \mathbf{C}(\lambda^*, \lambda^*) - \mathbf{C}(\lambda^*, D_m) \mathbf{C}_\phi^{-1} \mathbf{C}(D_m, \lambda^*). \quad (\text{C.2.6})$$

Equivalently,

$$\vec{\theta}^* = \vec{m}_\beta(\lambda^*) + \mathbf{C}(\lambda^*, D_m) \mathbf{C}_\phi^{-1} (\vec{\Theta}_m - \vec{M}_\beta) + \eta_{\text{cond}}, \quad (\text{C.2.7})$$

where  $\eta_{\text{cond}} \sim \mathcal{N}(0, \Sigma_{\text{cond}}(\lambda^*, \lambda^*))$  is independent of  $\vec{\Theta}_m$ . Since  $\pi(\vec{\Theta}_m | \vec{\mathbf{z}}, \phi)$  is Gaussian, integrating  $\pi(\vec{\theta}^* | \vec{\Theta}_m, \phi)$  with respect to this posterior yields a Gaussian distribution. By Theorem 1,

$$\vec{\Theta}_m | \vec{\mathbf{z}}, \phi \sim \mathcal{N}(\mu_\phi, \Sigma_\phi). \quad (\text{C.2.8})$$

Substituting  $\vec{\Theta}_m = \mu_\phi + (\vec{\Theta}_m - \mu_\phi)$  into Eq. (C.2.7) gives

$$\begin{aligned} \vec{\theta}^* | \vec{\mathbf{z}}, \phi = \vec{m}_\beta(\lambda^*) + \mathbf{C}(\lambda^*, D_m) \mathbf{C}_\phi^{-1} (\mu_\phi - \vec{M}_\beta) + \\ \mathbf{C}(\lambda^*, D_m) \mathbf{C}_\phi^{-1} (\vec{\Theta}_m - \mu_\phi) + \eta_{\text{cond}}. \end{aligned} \quad (\text{C.2.9})$$

Therefore  $\vec{\theta}^* | \vec{\mathbf{z}}, \phi$  is Gaussian with mean

$$\bar{\theta}_{\text{pred}}(\lambda^*) = \vec{m}_\beta(\lambda^*) + \mathbf{C}(\lambda^*, D_m) \mathbf{C}_\phi^{-1} (\mu_\phi - \vec{M}_\beta), \quad (\text{C.2.10})$$

which coincides with Eq. (51). Moreover,

$$\vec{\theta}^* - \bar{\theta}_{\text{pred}}(\lambda^*) = \mathbf{C}(\lambda^*, D_m) \mathbf{C}_\phi^{-1} (\vec{\Theta}_m - \mu_\phi) + \eta_{\text{cond}}. \quad (\text{C.2.11})$$

Using independence and zero means,

$$\Sigma_{\text{pred}}(\lambda^*, \lambda^*) = \mathbf{C}(\lambda^*, D_m) \mathbf{C}_\phi^{-1} \Sigma_\phi \mathbf{C}_\phi^{-1} \mathbf{C}(D_m, \lambda^*) + \Sigma_{\text{cond}}(\lambda^*, \lambda^*). \quad (\text{C.2.12})$$

For a general pair  $(\lambda^*, \lambda^{*'})$ , define

$$\Sigma_{\text{cond}}(\lambda^*, \lambda^{*'}) = \mathbf{C}(\lambda^*, \lambda^{*'}) - \mathbf{C}(\lambda^*, D_m) \mathbf{C}_\phi^{-1} \mathbf{C}(D_m, \lambda^{*'}). \quad (\text{C.2.13})$$

Then the predictive cross-covariance is given by

$$\Sigma_{\text{pred}}(\lambda^*, \lambda^{*'}) = \Sigma_{\text{cond}}(\lambda^*, \lambda^{*'}) + \mathbf{C}(\lambda^*, D_m) \mathbf{C}_\phi^{-1} \Sigma_\phi \mathbf{C}_\phi^{-1} \mathbf{C}(D_m, \lambda^{*'}). \quad (\text{C.2.14})$$

which is Eq. (52). This completes the proof.  $\square$

### C.3 Marginal likelihood expression and hyperparameters tuning

The hyperparameters  $\phi = \{(\beta_l, \sigma_l^2, \psi_l)\}_{l=1}^p$  are estimated by maximizing the marginal likelihood of the vectorized experimental data  $\vec{\mathbf{z}} \in \mathbb{R}^{nm}$ . Conditionally on  $\vec{\Theta}_m$ , the likelihood is given by

$$\mathcal{L}(\vec{\mathbf{z}} | \vec{\Theta}_m) \sim \mathcal{N}(\vec{\mathbf{z}}; G\vec{\Theta}_m, \Sigma_{\vec{\epsilon}}), \quad (\text{C.3.1})$$

while the prior distribution of  $\vec{\Theta}_m$  reads

$$\pi(\vec{\Theta}_m | \phi) \sim \mathcal{N}(\vec{\Theta}_m; \vec{M}_\beta, \mathbf{C}_\phi), \quad (\text{C.3.2})$$

where  $\mathbf{C}_\phi$  is assumed to be symmetric positive definite. The marginal likelihood is obtained by integrating out  $\vec{\Theta}_m$ :

$$\hat{\phi} = \operatorname{argmax}_{\phi} \int_{\mathcal{T}^m} \mathcal{L}(\vec{\mathbf{z}}|\vec{\Theta}_m) \pi(\vec{\Theta}_m|\phi) d\vec{\Theta}_m. \quad (\text{C.3.3})$$

Since the likelihood and the prior define a jointly Gaussian model in  $(\vec{\mathbf{z}}, \vec{\Theta}_m)$ , the marginal distribution of  $\vec{\mathbf{z}}$  is Gaussian and is obtained from standard linear-Gaussian marginalization formulas:

$$\pi(\vec{\mathbf{z}}|\phi) \sim \mathcal{N}\left(\vec{\mathbf{z}}; G\vec{M}_\beta, \Sigma_{\vec{\epsilon}} + G\mathbf{C}_\phi G^t\right). \quad (\text{C.3.4})$$

Define for convenience the marginal covariance matrix

$$\Sigma_{\mathbf{z}}(\phi) := \Sigma_{\vec{\epsilon}} + G\mathbf{C}_\phi G^t \in \mathbb{R}^{nm \times nm}. \quad (\text{C.3.5})$$

The marginal likelihood can therefore be written explicitly as

$$\pi(\vec{\mathbf{z}}|\phi) = \frac{\exp\left(-\frac{1}{2}(\vec{\mathbf{z}} - G\vec{M}_\beta)^t \Sigma_{\mathbf{z}}(\phi)^{-1} (\vec{\mathbf{z}} - G\vec{M}_\beta)\right)}{(2\pi)^{nm/2} |\Sigma_{\mathbf{z}}(\phi)|^{1/2}}. \quad (\text{C.3.6})$$

Taking logarithms yields

$$\log \pi(\vec{\mathbf{z}}|\phi) = -\frac{1}{2} \log |\Sigma_{\mathbf{z}}(\phi)| - \frac{1}{2} (\vec{\mathbf{z}} - G\vec{M}_\beta)^t \Sigma_{\mathbf{z}}(\phi)^{-1} (\vec{\mathbf{z}} - G\vec{M}_\beta) + \text{const}. \quad (\text{C.3.7})$$

For convenience, we introduce the negative marginal log-likelihood

$$\ell(\beta, \sigma^2, \psi) := -2 \log \pi(\vec{\mathbf{z}}|\phi), \quad (\text{C.3.8})$$

where the additive constant independent of  $\phi$  is omitted. Assume now that the prior mean has the linear form

$$\vec{M}_\beta = H\beta, \quad H \in \mathbb{R}^{pm \times q}, \quad \beta \in \mathbb{R}^q, \quad (\text{C.3.9})$$

with  $H$  of full column rank. Then the criterion becomes

$$\ell(\beta, \sigma^2, \psi) = \log |\Sigma_{\mathbf{z}}(\phi)| + (\vec{\mathbf{z}} - GH\beta)^t \Sigma_{\mathbf{z}}(\phi)^{-1} (\vec{\mathbf{z}} - GH\beta) + \text{const}, \quad (\text{C.3.10})$$

which shows that, for fixed  $(\sigma^2, \psi)$ , the dependence of  $\ell$  on  $\beta$  is entirely contained in a generalized least-squares quadratic form.

**Proposition 3.** *Assume that  $\vec{M}_\beta = H\beta$  with  $H \in \mathbb{R}^{pm \times q}$  of full column rank, and define*

$$\Sigma_{\mathbf{z}}(\phi) := \Sigma_{\vec{\epsilon}} + G\mathbf{C}_\phi G^t.$$

*Then, for fixed  $(\sigma^2, \psi)$ , the minimizer of  $\ell(\beta, \sigma^2, \psi)$  with respect to  $\beta$  is the generalized least-squares estimator*

$$\hat{\beta}(\sigma^2, \psi) = (H^t G^t \Sigma_{\mathbf{z}}(\phi)^{-1} GH)^{-1} H^t G^t \Sigma_{\mathbf{z}}(\phi)^{-1} \vec{\mathbf{z}}. \quad (\text{C.3.11})$$

### Proof of Proposition 3

*Proof.* For fixed  $(\sigma^2, \psi)$ , the marginal criterion

$$\ell(\beta, \sigma^2, \psi) = \log |\Sigma_{\mathbf{z}}(\phi)| + (\bar{\mathbf{z}} - GH\beta)^t \Sigma_{\mathbf{z}}(\phi)^{-1} (\bar{\mathbf{z}} - GH\beta) + \text{const}$$

depends on  $\beta$  only through the quadratic term. Minimizing  $\ell$  with respect to  $\beta$  is therefore equivalent to minimizing

$$Q(\beta) := (\bar{\mathbf{z}} - GH\beta)^t \Sigma_{\mathbf{z}}(\phi)^{-1} (\bar{\mathbf{z}} - GH\beta). \quad (\text{C.3.12})$$

Since  $\Sigma_{\mathbf{z}}(\phi)$  is symmetric positive definite,  $Q(\beta)$  is a strictly convex quadratic form in  $\beta$ . Taking the gradient with respect to  $\beta$  yields

$$\nabla_{\beta} Q(\beta) = -2 H^t G^t \Sigma_{\mathbf{z}}(\phi)^{-1} (\bar{\mathbf{z}} - GH\beta). \quad (\text{C.3.13})$$

The first-order optimality condition  $\nabla_{\beta} Q(\beta) = 0$  gives

$$H^t G^t \Sigma_{\mathbf{z}}(\phi)^{-1} GH \beta = H^t G^t \Sigma_{\mathbf{z}}(\phi)^{-1} \bar{\mathbf{z}}. \quad (\text{C.3.14})$$

Since  $H$  has full column rank and  $\Sigma_{\mathbf{z}}(\phi)$  is positive definite,  $H^t G^t \Sigma_{\mathbf{z}}(\phi)^{-1} GH$  is invertible. Hence the unique minimizer is

$$\hat{\beta}(\sigma^2, \psi) = (H^t G^t \Sigma_{\mathbf{z}}(\phi)^{-1} GH)^{-1} H^t G^t \Sigma_{\mathbf{z}}(\phi)^{-1} \bar{\mathbf{z}}, \quad (\text{C.3.15})$$

which concludes the proof.  $\square$

Based on Proposition 3, the estimation of the hyperparameters  $(\sigma^2, \psi)$  reduces to the optimization of the marginal criterion with the estimator  $\hat{\beta}(\sigma^2, \psi)$  plugged in:

$$(\hat{\sigma}^2, \hat{\psi}) = \underset{\sigma^2, \psi}{\text{argmin}} \ell(\hat{\beta}(\sigma^2, \psi), \sigma^2, \psi). \quad (\text{C.3.16})$$

The resulting profile objective function is

$$\begin{aligned} \ell(\hat{\beta}(\sigma^2, \psi), \sigma^2, \psi) &= \log |\Sigma_{\bar{\epsilon}} + G\mathbf{C}_{\phi}G^t| \\ &\quad + (\bar{\mathbf{z}} - G\vec{M}_{\hat{\beta}})^t (\Sigma_{\bar{\epsilon}} + G\mathbf{C}_{\phi}G^t)^{-1} (\bar{\mathbf{z}} - G\vec{M}_{\hat{\beta}}) \end{aligned} \quad (\text{C.3.17})$$

where  $\vec{M}_{\hat{\beta}} := H\hat{\beta}(\sigma^2, \psi)$ . The minimization with respect to  $(\sigma^2, \psi)$  is performed numerically.

**Remark** (Alternative expression of  $\hat{\beta}$ ). Assume in addition that the design matrix  $G$  has full column rank, so that  $\Delta^{-1} = G^t \Sigma_{\bar{\epsilon}}^{-1} G$  is invertible and  $\Delta$  is well-defined. Under the assumptions of Proposition 3, the estimator

$$\hat{\beta}(\sigma^2, \psi) = (H^t G^t \Sigma_{\mathbf{z}}(\phi)^{-1} GH)^{-1} H^t G^t \Sigma_{\mathbf{z}}(\phi)^{-1} \bar{\mathbf{z}}, \quad (\text{C.3.18})$$

with

$$\Sigma_{\mathbf{z}}(\phi) = \Sigma_{\bar{\epsilon}} + G\mathbf{C}_{\phi}G^t, \quad (\text{C.3.19})$$

admits the equivalent representation

$$\hat{\beta}(\sigma^2, \psi) = (H^t(\Delta + \mathbf{C}_{\phi})^{-1}H)^{-1}H^t(\Delta + \mathbf{C}_{\phi})^{-1}\Delta G^t\Sigma_{\bar{\epsilon}}^{-1}\bar{\mathbf{z}}, \quad (\text{C.3.20})$$

where

$$\Delta^{-1} = G^t\Sigma_{\bar{\epsilon}}^{-1}G. \quad (\text{C.3.21})$$

*Proof.* By Woodbury's identity applied to

$$\Sigma_{\mathbf{z}}(\phi) = \Sigma_{\bar{\epsilon}} + G\mathbf{C}_{\phi}G^t, \quad (\text{C.3.22})$$

we obtain

$$\Sigma_{\mathbf{z}}(\phi)^{-1} = \Sigma_{\bar{\epsilon}}^{-1} - \Sigma_{\bar{\epsilon}}^{-1}G(\mathbf{C}_{\phi}^{-1} + G^t\Sigma_{\bar{\epsilon}}^{-1}G)^{-1}G^t\Sigma_{\bar{\epsilon}}^{-1}. \quad (\text{C.3.23})$$

Using the definition

$$\Delta^{-1} = G^t\Sigma_{\bar{\epsilon}}^{-1}G, \quad (\text{C.3.24})$$

this expression can be rewritten as

$$\Sigma_{\mathbf{z}}(\phi)^{-1} = \Sigma_{\bar{\epsilon}}^{-1} - \Sigma_{\bar{\epsilon}}^{-1}G(\mathbf{C}_{\phi}^{-1} + \Delta^{-1})^{-1}G^t\Sigma_{\bar{\epsilon}}^{-1}. \quad (\text{C.3.25})$$

Substituting this expression into  $G^t\Sigma_{\mathbf{z}}(\phi)^{-1}$  yields

$$G^t\Sigma_{\mathbf{z}}(\phi)^{-1} = \left(I - \Delta^{-1}(\mathbf{C}_{\phi}^{-1} + \Delta^{-1})^{-1}\right)G^t\Sigma_{\bar{\epsilon}}^{-1}. \quad (\text{C.3.26})$$

We now show that

$$I - \Delta^{-1}(\mathbf{C}_{\phi}^{-1} + \Delta^{-1})^{-1} = (\Delta + \mathbf{C}_{\phi})^{-1}\Delta. \quad (\text{C.3.27})$$

Let

$$A := \mathbf{C}_{\phi}^{-1} + \Delta^{-1}. \quad (\text{C.3.28})$$

Since  $A$  is invertible, it is enough to prove that the two sides of Eq. (C.3.27) have the same product with  $A$  on the right. First,

$$\left(I - \Delta^{-1}A^{-1}\right)A = A - \Delta^{-1} = \mathbf{C}_{\phi}^{-1}. \quad (\text{C.3.29})$$

Second,

$$(\Delta + \mathbf{C}_{\phi})^{-1}\Delta A = (\Delta + \mathbf{C}_{\phi})^{-1}\Delta(\mathbf{C}_{\phi}^{-1} + \Delta^{-1}) \quad (\text{C.3.30})$$

$$= (\Delta + \mathbf{C}_{\phi})^{-1}(\Delta\mathbf{C}_{\phi}^{-1} + I) \quad (\text{C.3.31})$$

$$= (\Delta + \mathbf{C}_{\phi})^{-1}(\Delta + \mathbf{C}_{\phi})\mathbf{C}_{\phi}^{-1} \quad (\text{C.3.32})$$

$$= \mathbf{C}_{\phi}^{-1}. \quad (\text{C.3.33})$$

Therefore, Eq. (C.3.27) is established. Then, combining Eq. (C.3.26) and Eq. (C.3.27) gives

$$G^t \Sigma_{\mathbf{z}}(\phi)^{-1} = (\Delta + \mathbf{C}_\phi)^{-1} \Delta G^t \Sigma_{\vec{\epsilon}}^{-1}. \quad (\text{C.3.34})$$

Consequently,

$$H^t G^t \Sigma_{\mathbf{z}}(\phi)^{-1} = H^t (\Delta + \mathbf{C}_\phi)^{-1} \Delta G^t \Sigma_{\vec{\epsilon}}^{-1}, \quad (\text{C.3.35})$$

and

$$H^t G^t \Sigma_{\mathbf{z}}(\phi)^{-1} G H = H^t (\Delta + \mathbf{C}_\phi)^{-1} \Delta (G^t \Sigma_{\vec{\epsilon}}^{-1} G) H = H^t (\Delta + \mathbf{C}_\phi)^{-1} H. \quad (\text{C.3.36})$$

Replacing these expressions into Eq. (C.3.11) gives exactly Eq. (C.3.20), which concludes the proof.  $\square$

From a numerical standpoint, the estimator in Eq. (C.3.20) is advantageous when the dimension  $pm$  of  $\vec{\Theta}_m$  is small compared to the dimension  $nm$  of  $\vec{\mathbf{z}}$ . The generalized least-squares expression in Proposition 3 requires the inversion of the marginal covariance matrix  $\Sigma_{\mathbf{z}}(\phi) \in \mathbb{R}^{nm \times nm}$ , whereas the alternative formulation only involves the inversion of the matrix  $\Delta + \mathbf{C}_\phi \in \mathbb{R}^{pm \times pm}$ . This reduction in matrix size leads to a significant decrease in computational cost when  $n$  is large.